

SUPERFLUID DYNAMICS IN NEUTRON STARS

ALLARD Valentin

PhD private defense (*April 29, 2024*)



Faculty
of
Sciences



Table of contents

1 Context

- Superfluidity in the laboratory
- Nuclear superfluidity in neutron stars

2 Nuclear energy-density functional theory

- Formalism
- Exact solution in homogeneous superfluid nuclear matter

3 Gapless superfluidity

- Quasiparticle density of states and energy gap
- Specific heat
- Normal fluid

4 Astrophysical manifestation of gapless superfluidity

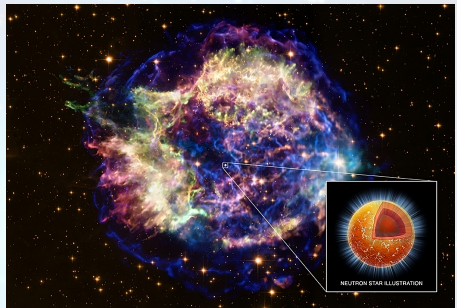
- Quasipersistent soft X-ray transients
- Cooling model
- Results

5 Conclusions and prospects

Neutron stars

Formed in gravitational core-collapse supernova explosions. **Predicted in 1933** (Baade and Zwicky) and **observed in 1967** (Bell and Hewish)

- **Radius:** $R_{\text{NS}} \sim 10 \text{ km}$,
- **Mass:** $M_{\text{NS}} \sim 1.4 M_{\odot}$,
- **Density:** $\rho_{\text{NS}} \sim 10^{15} \text{ g/cm}^3$,
- **Energy scale (MeV):** $1 \text{ MeV} = 10^{10} \text{ K}$.
- **Temperature:** Initially very hot ($T \sim 100 \text{ MeV}$) but **cool down** to $T \sim 0.1 \text{ MeV}$, within days.

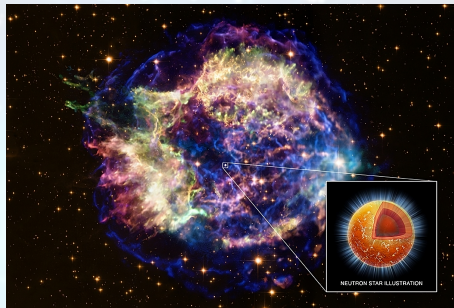


(Cassiopeia A, credits: NASA/CXC/SAO)

Neutron stars

Formed in gravitational core-collapse supernova explosions. **Predicted in 1933** (Baade and Zwicky) and **observed in 1967** (Bell and Hewish)

- **Radius:** $R_{\text{NS}} \sim 10 \text{ km}$,
- **Mass:** $M_{\text{NS}} \sim 1.4 M_{\odot}$,
- **Density:** $\rho_{\text{NS}} \sim 10^{15} \text{ g/cm}^3$,
- **Energy scale (MeV):** $1 \text{ MeV} = 10^{10} \text{ K}$.
- **Temperature:** Initially very hot ($T \sim 100 \text{ MeV}$) but **cool down** to $T \sim 0.1 \text{ MeV}$, within days.



(Cassiopeia A, credits: NASA/CXC/SAO)

Neutron stars contain **dense matter** which is expected to undergo various **phase transitions** such as **superfluidity**.

Superfluidity

First discovered in liquid ${}^4\text{He}$ (in the 1930's). Below the **critical temperature** $T_c \equiv T_\lambda = 2.17 \text{ K}$, helium does **not behave like an ordinary liquid**.



$$T > T_c$$

Superfluidity

First discovered in liquid ^4He (in the 1930's). Below the **critical temperature** $T_c \equiv T_\lambda = 2.17 \text{ K}$, helium does **not behave like an ordinary liquid**.



$$T \approx T_c$$

Superfluidity

First discovered in liquid ${}^4\text{He}$ (in the 1930's). Below the **critical temperature** $T_c \equiv T_\lambda = 2.17 \text{ K}$, helium does **not behave like an ordinary liquid**.



$$T < T_c$$

Superfluid ${}^4\text{He}$ does not boil \implies **Non classical heat transport**.

Superfluidity

First discovered in liquid ${}^4\text{He}$ (in the 1930's). Below the **critical temperature** $T_c \equiv T_\lambda = 2.17 \text{ K}$, helium does **not behave like an ordinary liquid**.



Superfluidity

First discovered in liquid ^4He (in the 1930's). Below the **critical temperature** $T_c \equiv T_\lambda = 2.17 \text{ K}$, helium does **not behave like an ordinary liquid**.



Superfluidity

First discovered in liquid ^4He (in the 1930's). Below the **critical temperature** $T_c \equiv T_\lambda = 2.17 \text{ K}$, helium does **not behave like an ordinary liquid**.

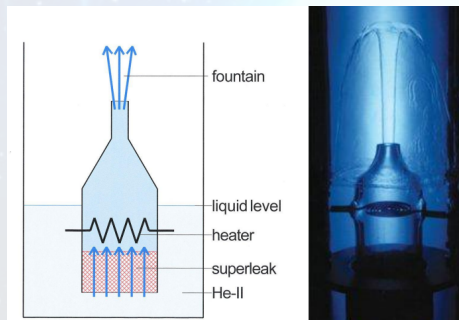


Flow without resistance through narrow slits and capillaries \implies **No viscosity**

Superfluid hydrodynamics

Tisza (1938) suggested that superfluid helium can be described by two interpenetrating "fluids" (Tisza, Nature, 141: 913 (1938)).

- A **superfluid**, carrying no entropy, with mass density $\rho^{(S)}$ and "Superfluid velocity" (momentum) V_S .
- A **normal viscous fluid**, carrying heat, with mass density $\rho^{(N)}$ and normal fluid velocity v_N .



(credit: Allen and Jones, Nature, 141:243 (1938))

Superfluid hydrodynamics

Tisza (1938) suggested that superfluid helium can be described by two interpenetrating "fluids" (Tisza, Nature, 141: 913 (1938)).

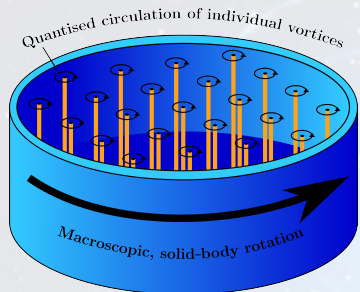
- A **superfluid**, carrying no entropy, with mass density $\rho^{(S)}$ and "Superfluid velocity" (momentum) V_S .
- A **normal** viscous **fluid**, carrying heat, with mass density $\rho^{(N)}$ and normal fluid velocity v_N .

Multifluid hydrodynamics

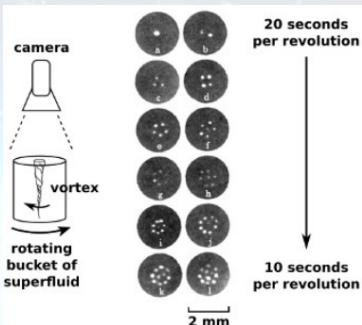
A superfluid contains **two** different **velocity fields** (Tisza, Nature 141, 913; Landau, Phys. Rev. 60, 356): V_S and v_N .

Superfluid hydrodynamics

A rotating superfluid is threaded by an **array of quantum vortices**.



(Gruber and Andersson, International Journal of Modern Physics D, Vol. 26, No. 08, 1730015 (2017)).

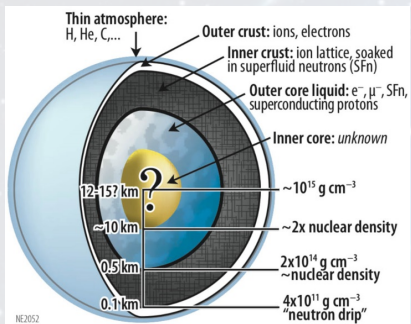


(Yarmchuk et al., Phys. Rev. Lett. 43:214–217 (1979)).

Spinning-up (spinning-down) the superfluid is achieved by creating (destroying) vortices.

Nuclear superfluidity in neutron stars

Nuclear superfluidity predicted well before the discovery of neutron stars.

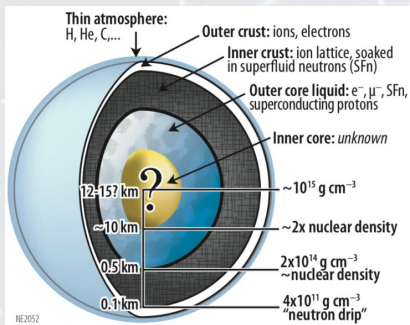


(credit: NASA, NICER Team)

- **Neutron superfluidity** in the inner crust and **neutron-proton superfluid mixture** in the core.
- Impact on transport and thermal properties.
- **Superfluid neutrons weakly coupled** to the rest of the star
⇒ **Superflows**.

Nuclear superfluidity in neutron stars

Nuclear superfluidity predicted well before the discovery of neutron stars.



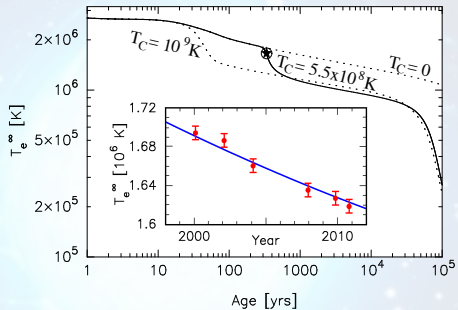
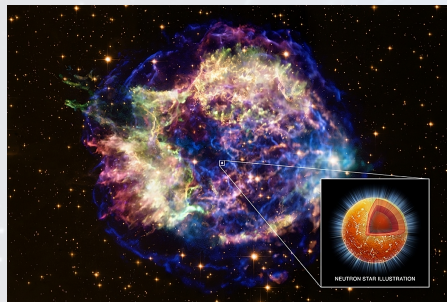
(credit: NASA, NICER Team)

- **Neutron superfluidity** in the inner crust and **neutron-proton superfluid mixture** in the core.
- Impact on transport and thermal properties.
- **Superfluid neutrons weakly coupled** to the rest of the star
⇒ **Superflows**.

Most microscopic studies consider the neutron superfluid co-moving with the rest of the star.

Evidence of neutron star superfluidity: Cassiopeia A

The fast cooling of the Cassiopeia A remnant suggests a recent transition to **Nuclear superfluidity**. (Page et al., Phys. Rev. Lett. 106, 081101; Shternin et al., MNRAS 412, L108; Ho et al., MNRAS 506, 5015; Posselt et al., Astrophys. J. 932, 83).



How do finite superflows influence the critical temperature T_c ?

Pulsar frequency glitches

Pulsars are rotating neutron stars spinning with stable periods ($\dot{P} \gtrsim 10^{-12}$)
BUT.

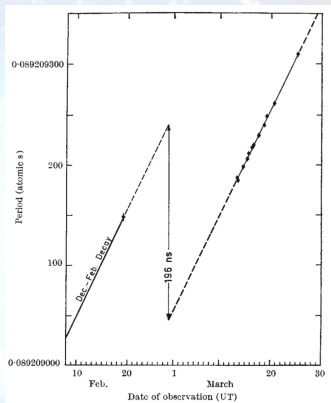
Pulsar glitches

Sudden decrease of spin period of pulsars (rotating NS) interpreted as the **manifestation of superfluid dynamics**.

(see, e.g. Antonopoulou et al., Reports on Progress in Physics, 85(12), 126901 (2022)).

So far, 672 glitches (in 225 pulsars) have been detected.

<http://www.jb.man.ac.uk/pulsar/glitches.html>

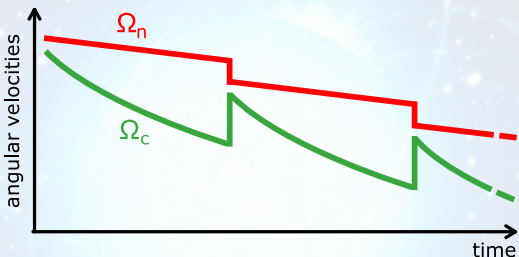


(Radhakrishnan and Manchester, Nature, 222:228–229 (1969))

Pulsar frequency glitches

Explained by a transfer of angular momentum between a superfluid component and a “normal” component (Anderson and Itoh, Nature, 256:25–27 (1975)).

- Superfluid component (rotating with Ω_n) threaded by quantized vortices.
- Normal component made of the (non-superfluid) crust and charged particles tightly coupled (rotating with Ω_c).



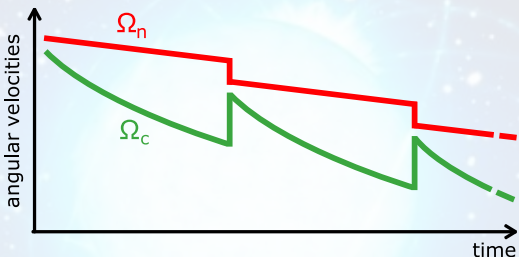
(Sourie et al., Phys. Rev. D. 93:083004 (2016))

Glitches triggered by catastrophic vortex unpinning caused by an increasing lag $\Omega_n - \Omega_c$.

Pulsar frequency glitches

Explained by a transfer of angular momentum between a superfluid component and a “normal” component (Anderson and Itoh, Nature, 256:25–27 (1975)).

- Superfluid component (rotating with Ω_n) threaded by quantized vortices.
- Normal component made of the (non-superfluid) crust and charged particles tightly coupled (rotating with Ω_c).



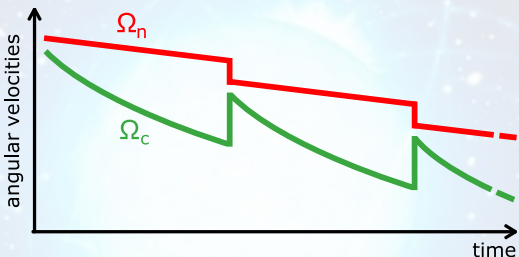
(Sourie et al., Phys. Rev. D. 93:083004 (2016))

The very long post-glitch relaxation (from days to years) also provided the evidence for superfluidity (Baym et al., Nature 224, 673 (1969)).

Pulsar frequency glitches

Explained by a transfer of angular momentum between a superfluid component and a “normal” component (Anderson and Itoh, Nature, 256:25–27 (1975)).

- Superfluid component (rotating with Ω_n) threaded by quantized vortices.
- Normal component made of the (non-superfluid) crust and charged particles tightly coupled (rotating with Ω_c).

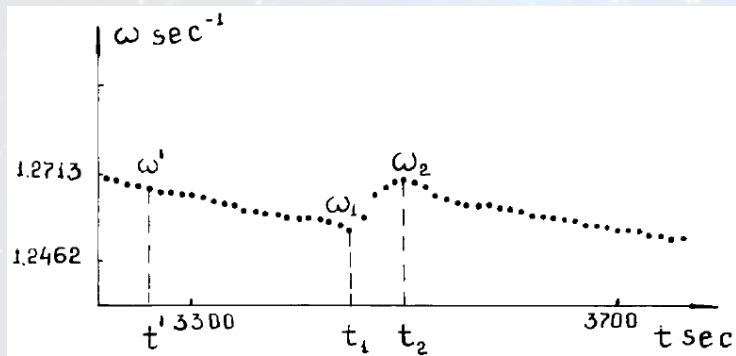


(Sourie et al., Phys. Rev. D, 93:083004 (2016))

Currents induced by the lag $\Omega_n - \Omega_c$ could exceed a critical value and destroy superfluidity (Sedrakian and Cordes, MNRAS, 307:365–375 (1999)).

Pulsar frequency glitches

Glitch-like behaviors have also been observed in laboratory experiments using containers filled with superfluid helium (Tsakadze and Tsakadze, J. Low Temp. Phys. 39 (1980)).



Glitches were also simulated using ultracold atoms (Poli et al., Phys. Rev. Lett. 131, 223401 (2023)).

Superfluid hydrodynamics and entrainment effects

Similarly to superfluid $^3\text{He}-^4\text{He}$ mixture (Andreev and Bashkin, Sov. Phys. JETP 42, 164 (1975)), **superfluid neutrons (n) and protons (p) in a neutron star** are mutually coupled by non-dissipative **entrainment effects** (Gusakov and Haensel, Nucl. Phys. A, 761:333–348 (2005)).

Mass current and velocity fields (superfluid mixtures)

Mass currents ρ_q (with $q = n, p$) are not simply aligned to their associated superfluid velocities V_q .

$$\rho_n = \rho_n^{(N)} v_N + \rho_{nn} V_n + \rho_{np} V_p ,$$

$$\rho_p = \rho_p^{(N)} v_N + \rho_{pp} V_p + \rho_{pn} V_n ,$$

$\rho_{qq'}$ = **Entrainment matrix** $\rho_q^{(N)}$ = **Normal density**

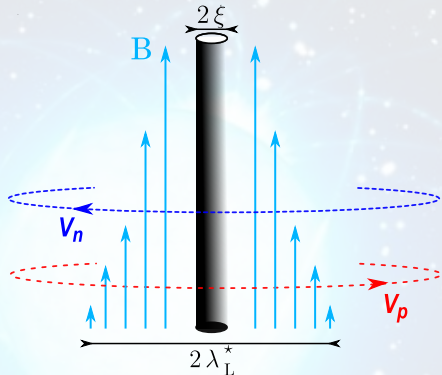
Superfluid hydrodynamics and entrainment effects

Entrainment effects induce a **circulation of protons around neutron vortices**.

Neutron vortices carry a magnetic flux Φ^* :

$$\Phi^* = \frac{hc}{2|e|} \frac{\rho_{np}}{\rho_{pp}}.$$

(Sedrakyan and Shakhabasyan, Astrofizika 8, 557 (1972); ibid. 16, 727 (1980))



Electrons scatter off the induced magnetic flux \Rightarrow strong coupling between the core superfluid and the crust (Alpar, Langer, Sauls, ApJ 282, 533 (1984)).

Aims

- Consistent determination of microscopic inputs for hydrodynamic simulations of superfluid neutron stars.

Aims

- Consistent determination of microscopic inputs for hydrodynamic simulations of superfluid neutron stars.
- Determination of critical velocities for the disappearance of superfluidity.

Aims

- Consistent determination of microscopic inputs for hydrodynamic simulations of superfluid neutron stars.
- Determination of critical velocities for the disappearance of superfluidity.
- Application to the cooling of transiently accreting neutron stars.

Energy-density functional theory

Why nuclear energy-density functional theory ?

- Self-consistent treatment of nuclear superfluidity in the crust and in the core.
- Previously used to compute the equation of state (see, for e.g. Potekhin et al, A&A, 560:A48 (2013), Fantina et al., A&A, 620: A105 (2018)).

Total **energy** $E(t)$ of a neutron-proton (superfluid) mixture = **functional** of various densities (e.g. $n_q(\mathbf{r}, t)$, $\tau_q(\mathbf{r}, t)$, $\tilde{n}_q(\mathbf{r}, t)$, ...) and currents (e.g. $\mathbf{j}_q(\mathbf{r}, t)$, ...) defined from the density $n_q(\mathbf{r}\sigma, \mathbf{r}'\sigma', t)$ and pair density matrices $\tilde{n}_q(\mathbf{r}\sigma, \mathbf{r}'\sigma', t)$.

In principle exact BUT the **exact functional** remains **to be determined**.

Energy-density functional theory

Minimizing $E(t)$ leads to the Time-dependent Hartree-Fock Bogoliubov (TDHFB) equations (highly **non-linear**):

$$i\hbar\partial_t n_q(\mathbf{r}\sigma, \mathbf{r}'\sigma', t) = h_q(\mathbf{r}, t)n_q(\mathbf{r}\sigma, \mathbf{r}'\sigma', t) - h_q^*(\mathbf{r}', t)n_q(\mathbf{r}\sigma, \mathbf{r}'\sigma', t) \\ + \sigma\sigma'\widetilde{\Delta}_q(\mathbf{r}, t)\tilde{n}_q(\mathbf{r} - \sigma, \mathbf{r}' - \sigma', t) - \tilde{n}_q(\mathbf{r}\sigma, \mathbf{r}'\sigma', t)\widetilde{\Delta}_q^\star(\mathbf{r}', t)$$

with the single-particle hamiltonian (depending on densities, **effective mass** and **currents**)

$$h_q(\mathbf{r}, t) = -\nabla \cdot \frac{\hbar^2}{2m_q^\oplus(\mathbf{r}, t)}\nabla + U_q(\mathbf{r}, t) + \frac{1}{2i}\left[\mathbf{I}_q(\mathbf{r}, t) \cdot \nabla + \nabla \cdot \mathbf{I}_q(\mathbf{r}, t)\right]$$

with potentials defined through various density and currents,

$$\frac{\hbar^2}{2m_q^\oplus(\mathbf{r}, t)} = \frac{\delta E}{\delta \tau_q(\mathbf{r}, t)}, \quad U_q(\mathbf{r}, t) = \frac{\delta E}{\delta n_q(\mathbf{r}, t)}, \quad \mathbf{I}_q(\mathbf{r}, t) = \frac{\delta E}{\delta \mathbf{j}_q(\mathbf{r}, t)},$$

Energy-density functional theory

Minimizing $E(t)$ leads to the Time-dependent Hartree-Fock Bogoliubov (TDHFB) equations (highly **non-linear**):

$$i\hbar\partial_t n_q(\mathbf{r}\sigma, \mathbf{r}'\sigma', t) = h_q(\mathbf{r}, t)n_q(\mathbf{r}\sigma, \mathbf{r}'\sigma', t) - h_q^*(\mathbf{r}', t)n_q(\mathbf{r}\sigma, \mathbf{r}'\sigma', t) \\ + \sigma\sigma'\widetilde{\Delta}_q(\mathbf{r}, t)\tilde{n}_q(\mathbf{r} - \sigma, \mathbf{r}' - \sigma', t) - \tilde{n}_q(\mathbf{r}\sigma, \mathbf{r}'\sigma', t)\widetilde{\Delta}_q^\star(\mathbf{r}', t)$$

with the (complex) **pairing field**

$$\widetilde{\Delta}_q(\mathbf{r}, t) = 2 \frac{\delta E}{\delta \tilde{n}_q^\star(\mathbf{r}, t)} = \Delta_q(\mathbf{r}, t)e^{i\phi_q(\mathbf{r}, t)},$$

whose phase $\phi_q(\mathbf{r}, t)$ is related to the **superfluid velocity**

$$\mathbf{V}_q = \frac{\hbar\nabla\phi_q}{2m_q}.$$

The quantity Δ_q corresponds to the pairing gap and is related to the order parameter of the superfluidity $\Psi_q \propto \Delta_q$!

Mass currents

A **continuity equation** can be derived from the TDHFB equations (Allard and Chamel in Phys. Rev. C. 100, 065801 (2019) and Phys. Rev. C. 103, 025804 (2021)) and gives the mass current $\rho_{\mathbf{q}}(\mathbf{r}, t)$

$$\rho_{\mathbf{q}}(\mathbf{r}, t) = \hbar j_{\mathbf{q}}(\mathbf{r}, t) \frac{m_q}{m_q^{\oplus}(\mathbf{r}, t)} + m_q n_q(\mathbf{r}, t) \frac{I_{\mathbf{q}}(\mathbf{r}, t)}{\hbar},$$

which:

- Does not explicitly depend on the pairing field $\tilde{\Delta}_q$.
- **General expression:** valid for both uniform and non-uniform systems.

Homogeneous solutions

Focusing on hot **homogeneous neutron-proton superfluid mixture** with stationary flows in normal fluid rest frame ($\mathbf{v}_N = 0$), **TDHFB can be solved exactly** (Allard and Chamel, Phys. Rev. C. 103, 025804 (2021)) !

Philosophy of the TDHFB equations

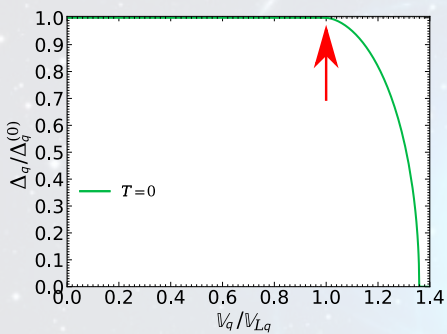
Strongly interacting particles \Rightarrow **weakly interacting quasiparticles** characterized by a quasiparticle energy $\mathcal{E}_k^{(q)}$ which depends on T and on the **effective superfluid velocity \mathbb{V}_q** .

Effective superfluid velocity

\mathbb{V}_q contains the mutual contributions of \mathbf{V}_n and \mathbf{V}_p and induces a **dynamical decoupling** between quantities associated with protons or neutrons !

Pairing gaps: finite T and finite currents

The pairing gap $\Delta_q(T, \mathbb{V}_q)$ is **universal after proper rescaling** (with velocity dependency entirely contained in the norm of \mathbb{V}_q).



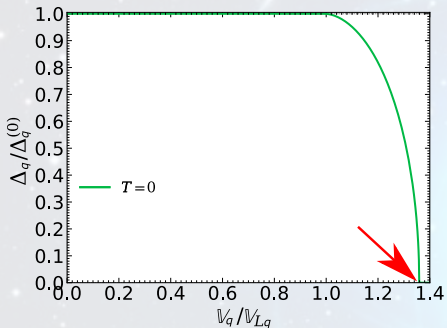
- $\Delta_q^{(0)}$ = Pairing gap at $T = 0$ and for $\mathbb{V}_q = 0$.

Approximate expressions

- $\mathbb{V}_{Lq} \approx \Delta_q^{(0)} / (\hbar k_{Fq})$ (**Landau's velocity**).

Pairing gaps: finite T and finite currents

The pairing gap $\Delta_q(T, \mathbb{V}_q)$ is **universal after proper rescaling** (with velocity dependency entirely contained in the norm of \mathbb{V}_q).



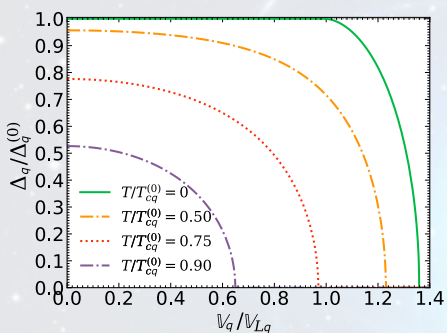
- $\Delta_q^{(0)}$ = Pairing gap at $T = 0$ and for $\mathbb{V}_q = 0$.

Approximate expressions

- $\mathbb{V}_{Lq} \approx \Delta_q^{(0)} / (\hbar k_{Fq})$ (**Landau's velocity**).
- Transition to normal phase beyond $\mathbb{V}_{cq}^{(0)} \simeq e\mathbb{V}_{Lq}/2$

Pairing gaps: finite T and finite currents

The pairing gap $\Delta_q(T, \mathbb{V}_q)$ is **universal after proper rescaling** (with velocity dependency entirely contained in the norm of \mathbb{V}_q).



- $\Delta_q^{(0)}$ = Pairing gap at $T = 0$ and for $\mathbb{V}_q = 0$.

Approximate expressions

- $\mathbb{V}_{Lq} \approx \Delta_q^{(0)} / (\hbar k_{Fq})$ (**Landau's velocity**).
- $\mathbb{V}_{cq}^{(0)} \approx e \mathbb{V}_{Lq} / 2$ (Critical velocity).
- $k_B T_{cq}^{(0)} \approx e^\gamma \Delta_q^{(0)} / \pi$ (BCS).

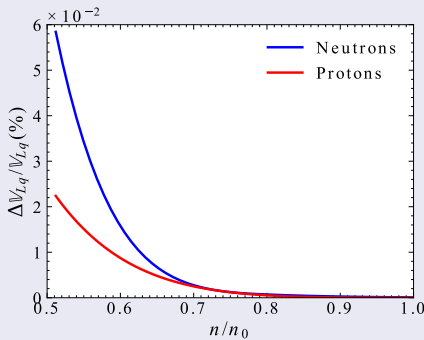
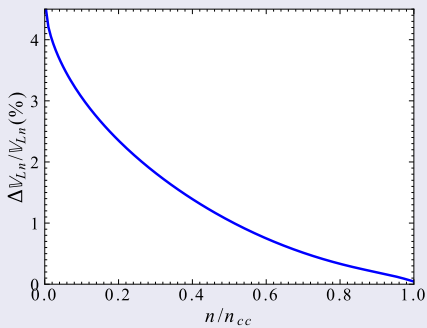
Approximate expressions and superfluid mixtures

Approximate expressions of the critical temperature and currents remain **valid for superfluid mixtures** (V. Allard and N. Chamel, Universe 7(12) (2021)) !

Critical velocities and approximations

Landau's velocity \mathbb{V}_{Lq} (at $T = 0$)

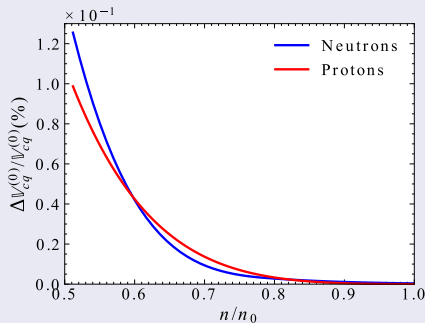
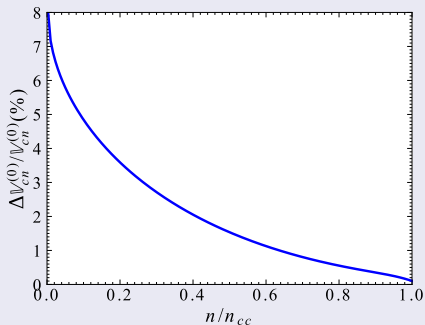
Threshold velocity beyond which Δ_q decreases.



Critical velocities and approximations

Critical velocity $\mathbb{V}_{cq}^{(0)}$ (at $T = 0$)

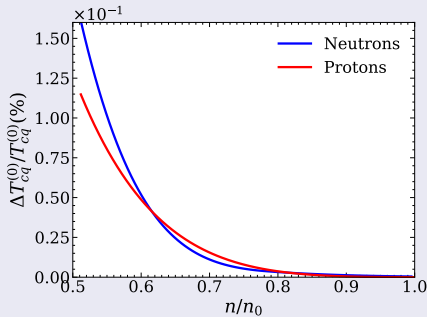
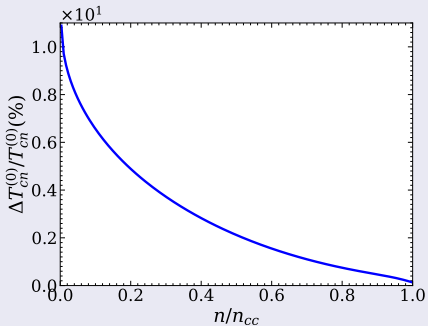
Destruction of superfluid phase (i.e. $\Delta_q = 0$).



Critical temperatures and approximations

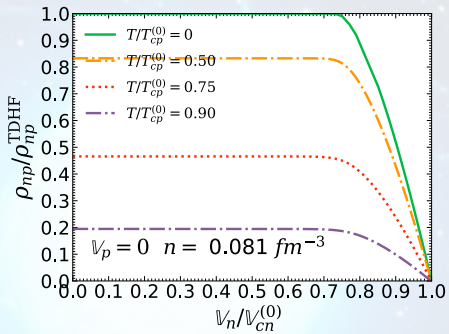
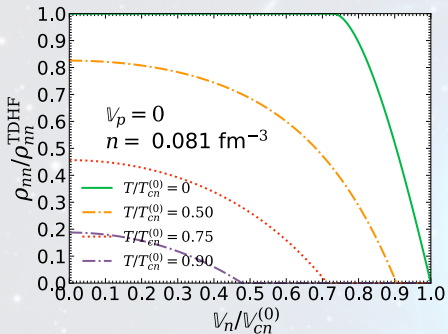
Critical temperature $T_{cq}^{(0)}$ (at $\mathbb{V}_q = 0$)

Destruction of superfluid phase (i.e. $\Delta_q = 0$).



Entrainment matrix: finite T and finite currents

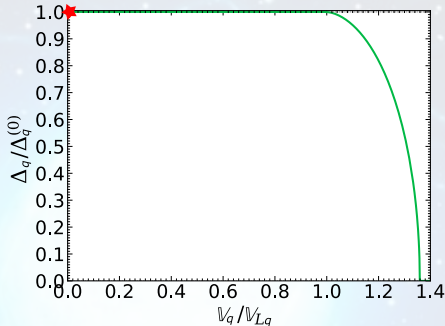
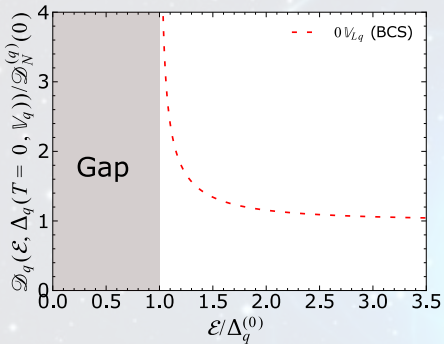
Entrainment matrix exactly computed in Allard and Chamel, Universe 7(12) (2021).



The entrainment matrix is the generalization of the **superfluid mass densities** for mixtures !

Energy gap and quasiparticle density of states

Finite currents influence the quasiparticle density of states (DoS).

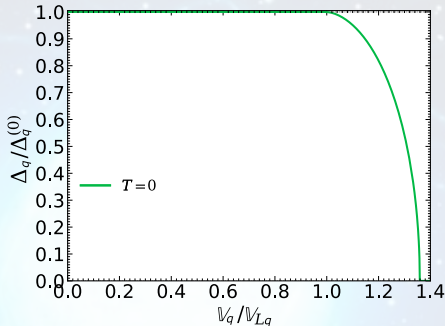
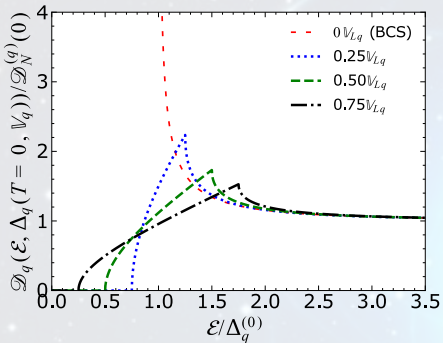


BCS regime: $V_q = 0$

No quasiparticle excitation for $\mathcal{E} < \Delta_q^{(0)}$ (**energy gap**).

Energy gap and quasiparticle density of states

Finite currents influence the quasiparticle density of states (DoS).

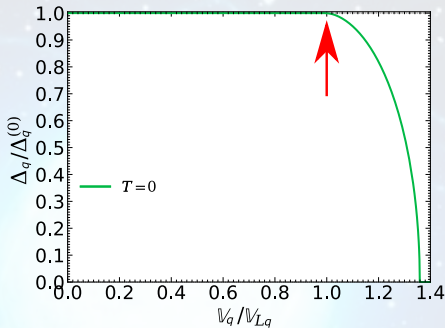
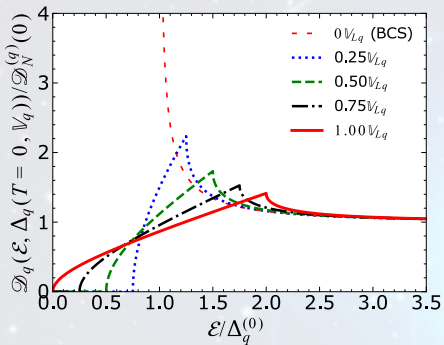


Subgapless regime: $\mathbb{V}_q < \mathbb{V}_{Lq}$

The energy gap shrinks with increasing \mathbb{V}_q (while $\Delta_q = \Delta_q^{(0)}$).

Energy gap and quasiparticle density of states

The gap disappears at Landau's velocity !



Gapless regime (Allard and Chamel, Phys. Rev. C. 108, 015801 (2023))

- **Gapless superfluidity ($\Delta_q \neq 0$) for $V_{Lq} \leq V_q \leq eV_{Lq}/2$.**
- **Impact on thermal properties** (e.g. the specific heat) !

Shrinking energy gap and specific heat

The presence of an **energy gap influences the specific heat**.

Normal phase: $\Delta_q = 0$ & $V_q = 0$

Specific heat proportional to the temperature:

$$c_N^{(q)}(T) \propto k_B^2 T$$

Shrinking energy gap and specific heat

The presence of an **energy gap influences the specific heat**.

Normal phase: $\Delta_q = 0$ & $\nabla_q = 0$

Specific heat proportional to the temperature:

$$c_N^{(q)}(T) \propto k_B^2 T$$

BCS superfluidity: $\Delta_q \neq 0$ & $\nabla_q = 0$

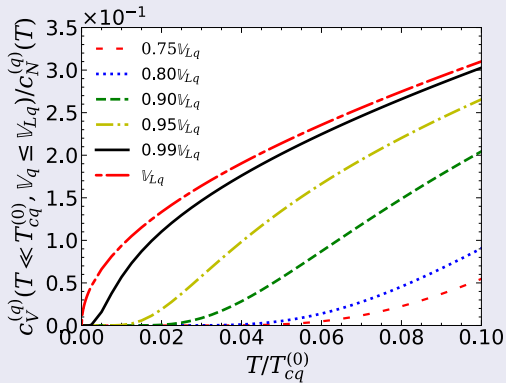
Exponential suppression at low temperatures:

$$c_V^{(q)}(T \ll T_{cq}^{(0)}) \propto e^{-\Delta_n^{(0)}/(k_B T)} c_N^{(q)}(T)$$

Shrinking energy gap and specific heat

Superfluid with finite velocities: $0 < \mathbb{V}_q \leq \mathbb{V}_{Lq}$

Increasing specific heat as the energy gap shrinks (with increasing \mathbb{V}_q).

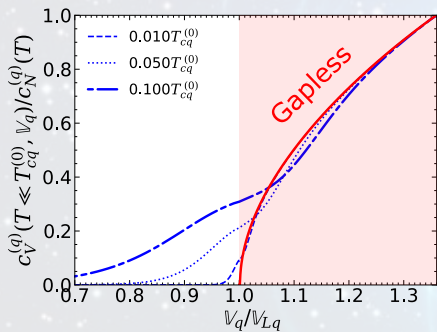


At \mathbb{V}_{Lq} : Exponential suppression \rightarrow Power-law suppression

Shrinking energy gap and specific heat

Gapless superfluidity: $\mathbb{V}_{Lq} < \mathbb{V}_q \leq e\mathbb{V}_{Lq}/2$

The specific heat $c_V^{(q)}$ becomes comparable to $c_N^{(q)}(T)$.

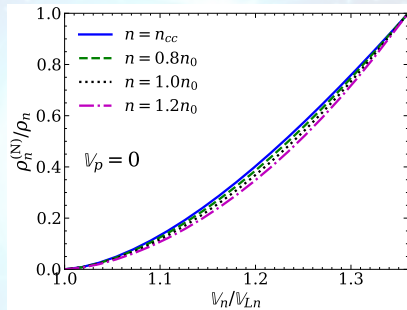
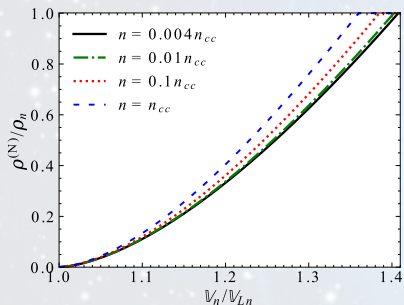


Universal expression for $c_V^{(q)}(T, \mathbb{V}_q) / c_N^{(q)}(T)$ as a function of $\mathbb{V}_q / \mathbb{V}_{Lq}$ (Allard and Chamel, Phys. Rev. C. 108, 015801 (2023)).

$$c_V^{(q)} / c_N^{(q)} = \sqrt{1 - \left(\frac{\Delta_q}{\Delta_q^{(0)}} \frac{\mathbb{V}_{Lq}}{\mathbb{V}_q} \right)^2}.$$

Normal fluid

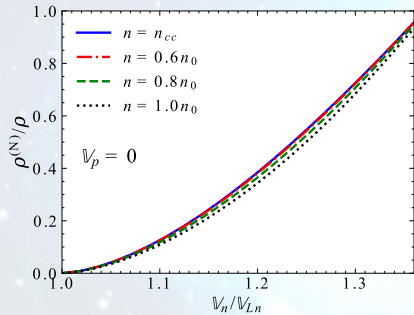
In gapless regime, the superfluid coexists with a **normal fluid** of quasiparticle excitations, $\rho^{(N)}$ (which depends on the entrainment matrix $\rho_{qq'}$).



Normal fluid fractions exactly computed in Allard and Chamel, Phys. Rev. C 108, 045801 (2023).

Normal fluid

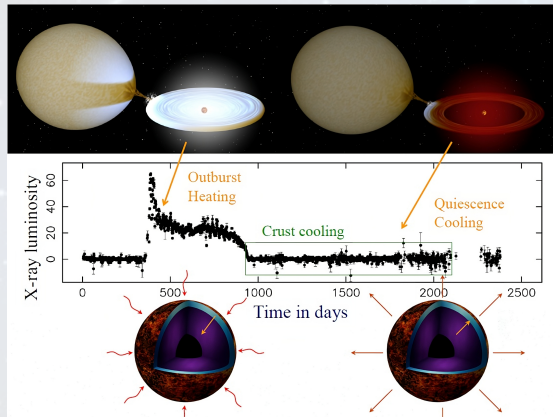
In gapless regime, the superfluid coexists with a **normal fluid** of quasiparticle excitations, $\rho^{(N)}$ (which depends on the entrainment matrix $\rho_{qq'}$).



Normal fluid fractions exactly computed in Allard and Chamel, Phys. Rev. C 108, 045801 (2023).

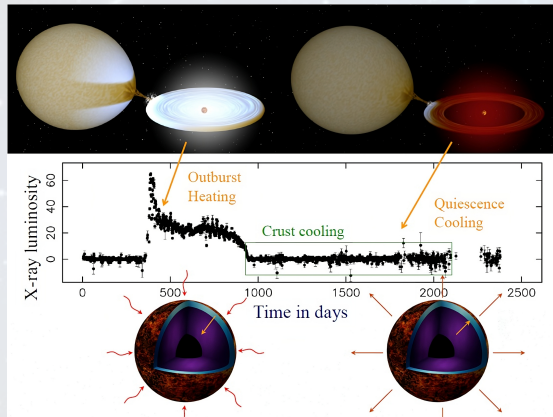
Application: Quasipersistent soft X-ray transients

Neutron star crust heated during **accretion regime** (for $\sim 1\text{-}10$ years) before **cooling phase** (Wijnands et al., J. Astrophys. Astr. 38: 49 (2017)).



Application: Quasipersistent soft X-ray transients

Neutron star crust heated during **accretion regime** (for $\sim 1\text{-}10$ years) before **cooling phase** (Wijnands et al., J. Astrophys. Astr. 38: 49 (2017)).



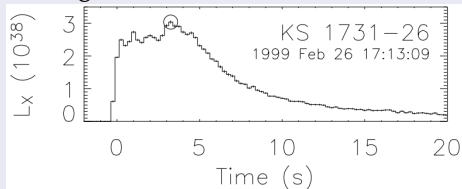
Thermal relaxation **observed for several sources** up to 10^4 days.

Crustal heating

During accretion, light elements (H and He) are accumulated on the neutron star surface. Formation of a stratified envelope.

X-ray bursts

Explosive **thermonuclear burning** and He fusion \Rightarrow sharp increase of X-ray luminosity lasting ~ 10 s, with recurrence time \sim hours-days.



(Galloway et al., *Astrophys. J. Suppl. S.*, 179:360 (2008))

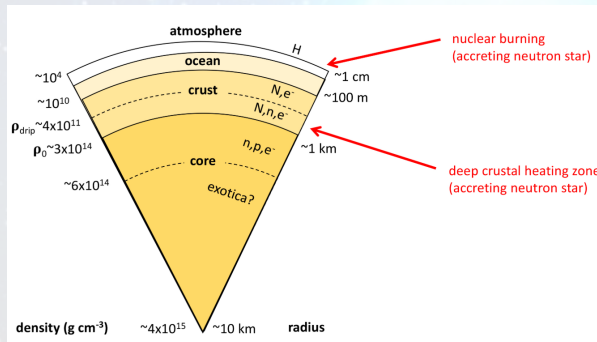
Production of nuclear ashes (mainly composed of Fe) and with a (small) amount of He BUT the **transition between Fe and He in the envelope is uncertain.**

Crustal heating

The newly-accreted material push the ashes in the neutron star interior.

Deep crustal heating

Compression-driven exothermic nuclear reactions heating the inner crust, releasing $Q_{\text{dch}} \sim 1.5 \text{ MeV/nucleon}$ (see, for e.g., Haensel & Zdunik, Astron. Astrophys. 227(2), 431–436 (1990) and Fantina et al., Astron. Astrophys. 620, 105 (2018)).



(Degenaar and Suleimanov, arxiv:1806.02833 (2018))

Crustal heating

Clusters are assumed to sink with the neutrons they emit or capture \Rightarrow non-physical jumps of the neutron chemical potential (local inconsistencies).

Neutron diffusion

Neutrons redistribute themselves between the different layers of the crust
(Gusakov et Chugunov Phys. Rev. Lett. 124, 191101 (2020) and Phys. Rev. D. 103, L101301 (2021)):

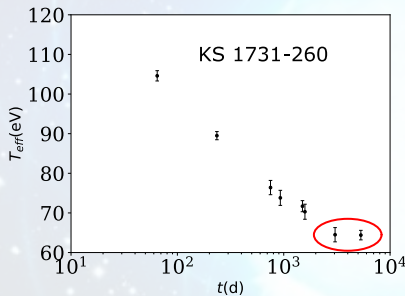
- **Modification of the crust equation of state** (close to the one obtained for non-accreted neutron stars).
- The **nuclear heating** is considerably **reduced** from $Q_{\text{dch}} \sim 1.5 \text{ MeV/nucleon}$ to $Q_{\text{nHD}} \sim 0.3 \text{ MeV/nucleon}$.

Problematic systems

Two systems **challenge our current understanding**:

KS 1731-260

- Colder than expected (Cackett et al., *Astrophys. J. Lett.*, 722: L137 (2010)).

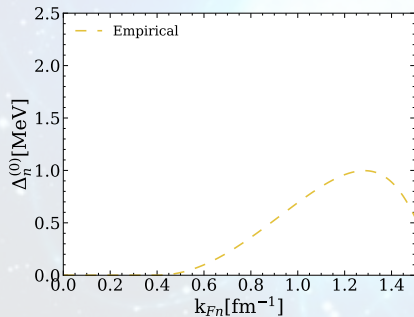


Problematic systems

Two systems **challenge our current understanding**:

KS 1731-260

- Colder than expected (Cackett et al., *Astrophys. J. Lett.*, 722: L137 (2010)).
- **Empirical** neutron pairing gap inferred from its cooling (Turlione et al., *A&A*, 577: A5 (2015)).

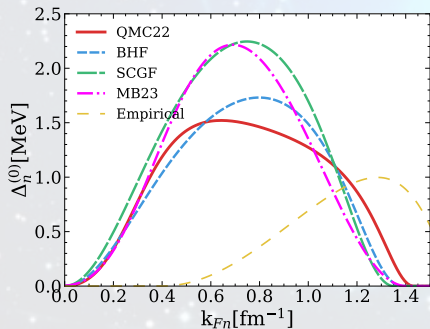


Problematic systems

Two systems **challenge our current understanding**:

KS 1731-260

- Colder than expected (Cackett et al., *Astrophys. J. Lett.*, 722: L137 (2010)).
- **Empirical** neutron pairing gap inferred from its cooling (Turrlione et al., *A&A*, 577: A5 (2015)) **BUT contradicted by microscopic results**.



Microscopic neutron pairing

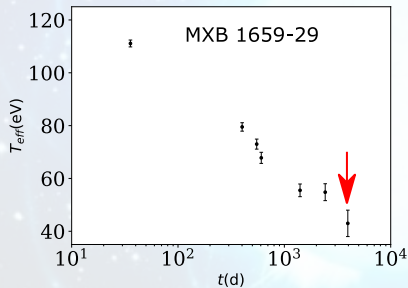
- **QMC22:** Gandolfi et al, *Condens. Matter*, 7(1) (2022).
- **BHF:** Cao et al., *Phys. Rev. C*, 73:014313 (2006).
- **SCGF:** Drissi and Rios, *Eur. Phys. J. A*, 58:90 (2022).
- **MB23:** Krotscheck et al, *Astrophys. J.*, 955: 76 (2023).

Problematic systems

Two systems **challenge our current understanding**:

MXB 1659-29

- **Unexpected** late-time temperature drop (Cackett et al., *Astrophys. J.*, 774: 131 (2013)).

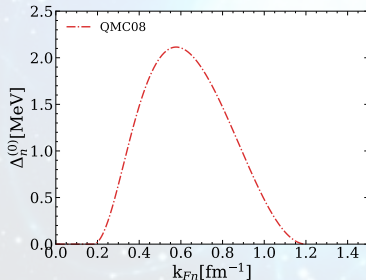


Problematic systems

Two systems **challenge our current understanding**:

MXB 1659-29

- **Unexpected** late-time temperature drop (Cackett et al., *Astrophys. J.*, 774: 131 (2013)).
- Neutrons in normal phase at high densities (Deibel et al., *Astrophys. J.*, 839: 95 (2017); Gandolfi et al., *Phys. Rev. Lett.* 101: 132501 (2008)).

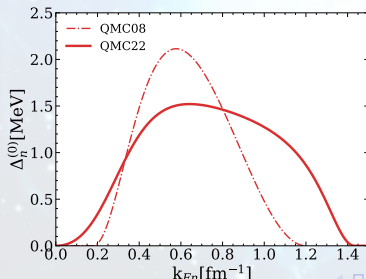


Problematic systems

Two systems **challenge our current understanding**:

MXB 1659-29

- **Unexpected late-time temperature drop** (Cackett et al., *Astrophys. J.*, 774: 131 (2013)).
- Neutrons in normal phase at high densities (Deibel et al., *Astrophys. J.* **839** (2017); Gandolfi et al., *Phys. Rev. Lett.* 101: 132501 (2008)) **BUT contradicted by recent results from the same group** (Gandolfi et al., *Condensed Matter*, 7 (2022)) !

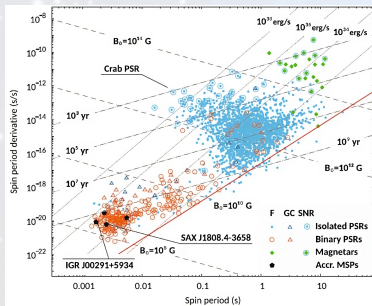


Origin of the relative flow in neutron stars

Previous cooling studies ignored neutron superflow BUT...

Recycling scenario (M. A., Alpar et al., Nature, 300:728 (1982))

Transfer of angular momentum from infalling material spinning up the crust
⇒ V_n increasing.



(credits: Alessandro Papitto)

Accreting millisecond X-ray pulsars ?

Burst oscillations likely related to neutron star spin. (see, e.g; Wijnands et al, *Astrophys. J.*, 549: L71–L75 (2001); *Astrophys. J.*, 594: 952–960 (2003) and Smith et al, *Astrophys. J.*, 479: L137–L140 (1997))

- KS 1731–260: $\nu_s \sim 524$ Hz.
- MXB 1659–29: $\nu_s \sim 567$ Hz.

Crustcool code

Study of the thermal evolution using crustcool (A. Cummings).

- Same microphysics as Brown et al., *Astrophys. J.*, 698: 1020–1032 (2009) BUT
- Modified neutron specific heat & parameterized with V_n + Approximate formula for the critical velocities.
- Implementation of neutron diffusion.

Crustcool code

Study of the thermal evolution using crustcool (A. Cummings).

- Same microphysics as Brown et al., *Astrophys. J.*, 698: 1020–1032 (2009) BUT
- Modified neutron specific heat & parameterized with \mathbb{V}_n + Approximate formula for the critical velocities.
- Implementation of neutron diffusion.

Parameters

- Accretion duration $t_{\text{accretion}}$ and accretion rate \dot{m} .
- Neutron star mass M_{NS} and radius R_{NS} .
- Core temperature (at thermal equilibrium) T_{core} and temperature at the basis of the envelope T_{base} .
- Impurity parameter Q_{imp} entering the thermal conductivity.
- (Effective) superfluid velocity \mathbb{V}_n entering the neutron specific heat.

Crustcool code

Study of the thermal evolution using crustcool (A. Cummings).

- Same microphysics as Brown et al., *Astrophys. J.*, 698: 1020–1032 (2009) BUT
- Modified neutron specific heat & parameterized with \mathbb{V}_n + Approximate formula for the critical velocities.
- Implementation of neutron diffusion.

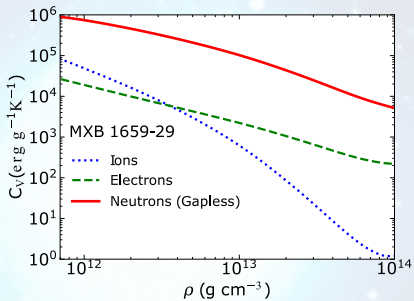
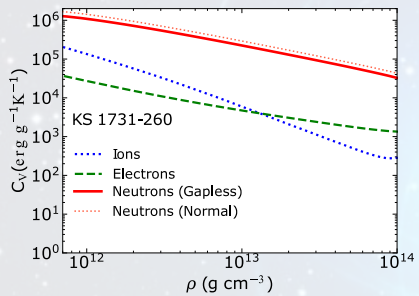
Parameters

- Accretion duration $t_{\text{accretion}}$ and accretion rate \dot{m} .
- Neutron star mass M_{NS} and radius R_{NS} .
- Core temperature (at thermal equilibrium) T_{core} and temperature at the basis of the envelope T_{base} .
- Impurity parameter Q_{imp} entering the thermal conductivity.
- (Effective) superfluid velocity \mathbb{V}_n entering the neutron specific heat.

Fixed $t_{\text{accretion}}$, \dot{m} , M_{NS} and R_{NS} and $(\mathbb{V}_n, T_{\text{core}}, T_{\text{base}}, Q_{\text{imp}})$ being free parameters.

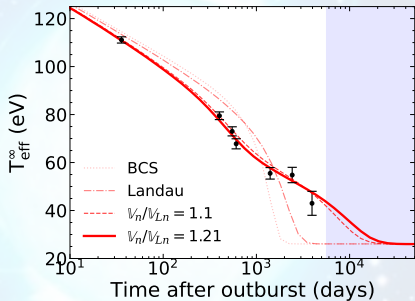
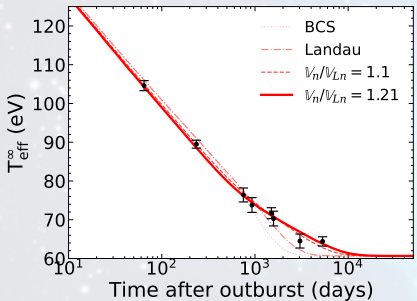
Cooling of the crust within gapless superfluidity

Gapless neutrons give the major contribution to the specific heat.



Cooling of the crust within gapless superfluidity

Gapless superfluidity allows to **explain observations using recent/realistic nuclear pairing (e.g., QMC22, BHF or SCGF)!**



Delayed thermal relaxation in the crust (Allard and Chamel, Phys. Rev. Lett. *in press* (2024)).

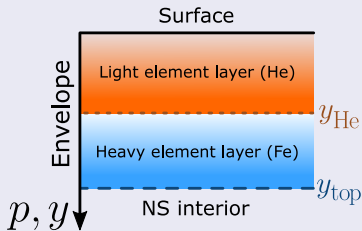
Neutron diffusion and gapless superfluidity

Uncertainties on M_{NS} and R_{NS}

Cooling simulations performed for a neutron star with $M_{\text{NS}} = 1.40M_{\odot}$, $R_{\text{NS}} = 10.0 \text{ km}$ and $M_{\text{NS}} = 1.62M_{\odot}$, $R_{\text{NS}} = 11.2 \text{ km}$.

Uncertainties on the envelope

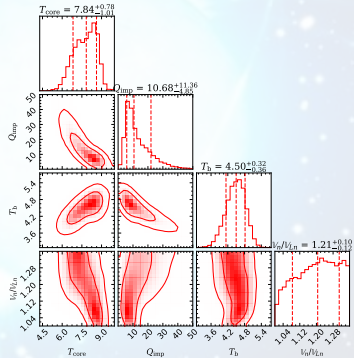
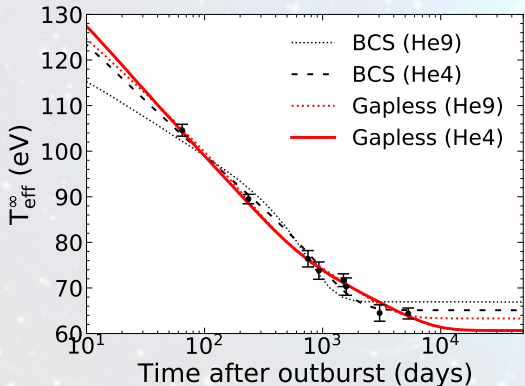
Cooling simulations performed for a light element (He9) and a heavy element (He4) envelope model (both are provided with the Crustcool code).



Neutron diffusion and gapless superfluidity

Cooling of KS 1731–260

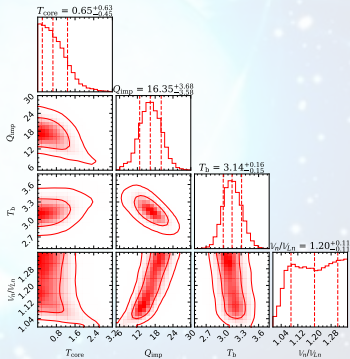
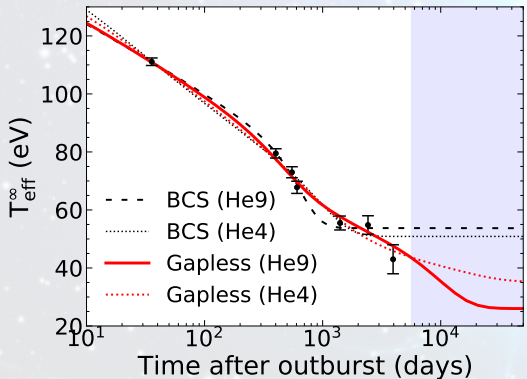
The NS with $M_{\text{NS}} = 1.40M_{\odot}$, $R_{\text{NS}} = 10.0$ km using the He4 envelope model, for neutrons in gapless regime, provides the best fit to the cooling data.



Neutron diffusion and gapless superfluidity

Cooling of MXB 1659–29 (outburst I)

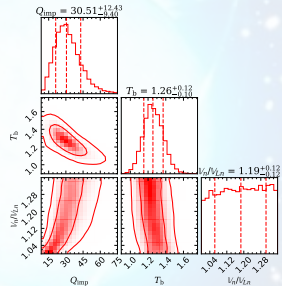
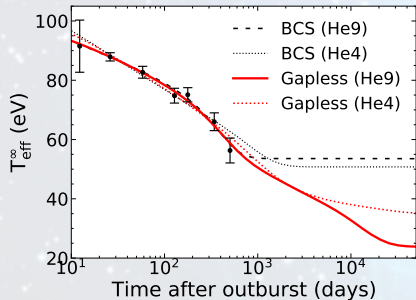
The NS with $M_{\text{NS}} = 1.62M_{\odot}$, $R_{\text{NS}} = 11.2$ km using the He9 envelope model, for neutrons in gapless regime, provides the best fit to the cooling data.



Neutron diffusion and gapless superfluidity

Cooling of MXB 1659–29 (outburst II)

The NS with $M_{\text{NS}} = 1.62M_{\odot}$, $R_{\text{NS}} = 11.2$ km using the He9 envelope model, for neutrons in gapless regime, provides the best fit to the cooling data.

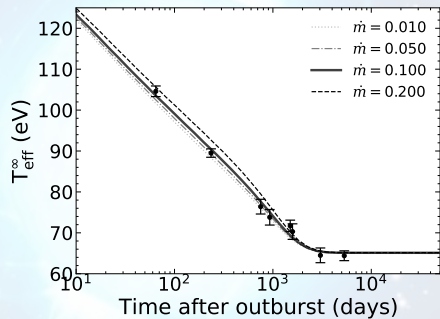
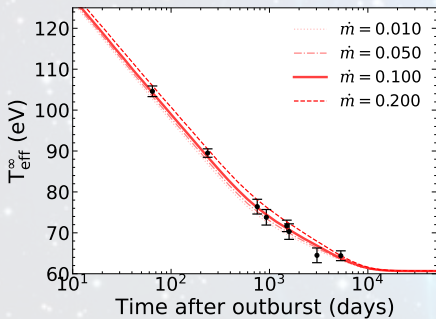


According to this model, MXB 1659–29 is still cooling.

Sensitivity to the mass accretion rate \dot{m}

Cooling has also been studied varying the (time-averaged) accretion rate \dot{m} .

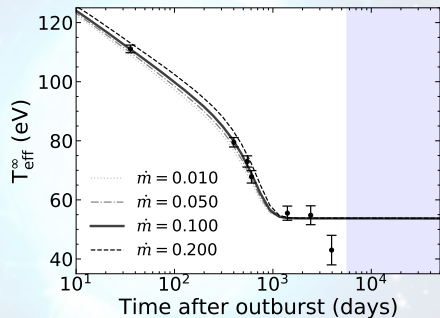
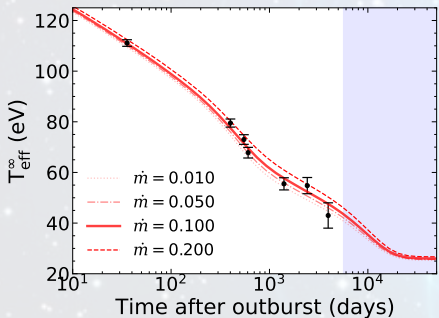
The impact of the uncertainties in \dot{m} on the cooling curves is of the same order as the errors associated with the observational data



Sensitivity to the mass accretion rate \dot{m}

Cooling has also been studied varying the (time-averaged) accretion rate \dot{m} .

The impact of the uncertainties in \dot{m} on the cooling curves is of the same order as the errors associated with the observational data

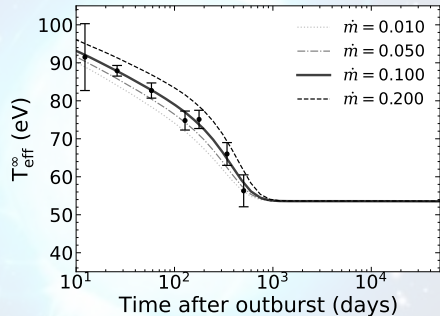
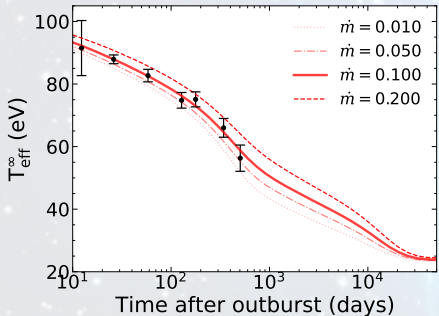


Changing \dot{m} does not explain the last observation point !

Sensitivity to the mass accretion rate \dot{m}

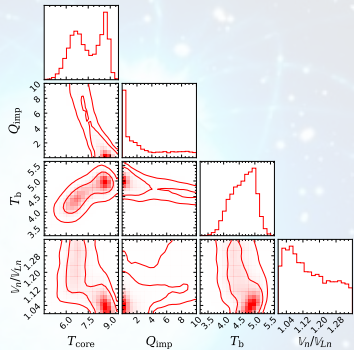
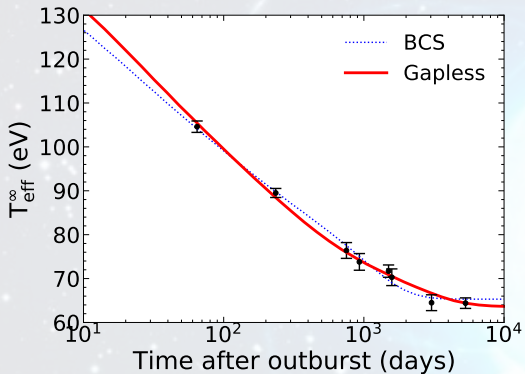
Cooling has also been studied varying the (time-averaged) accretion rate \dot{m} .

The impact of the uncertainties in \dot{m} on the cooling curves is of the same order as the errors associated with the observational data



Cooling with thermodynamically consistent EoS

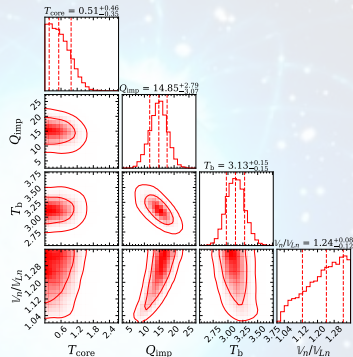
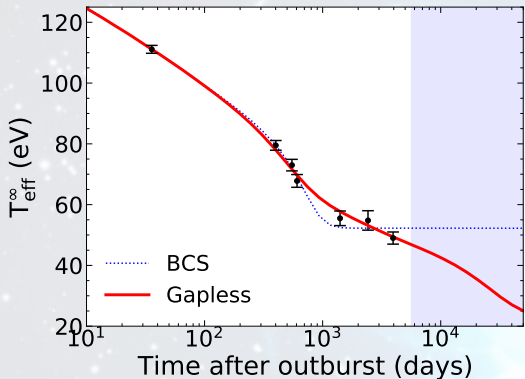
Cooling has been studied with a realistic equation of state of neutron matter based on BSk24 (following Potekhin et al. MNRAS 522:4830–4840 (2023)).



Both regime provide good fit to data and suggest low Q_{imp} (consistent with Shternin et al. MNRAS, 382: L43–L47 (2007)).

Cooling with thermodynamically consistent EoS

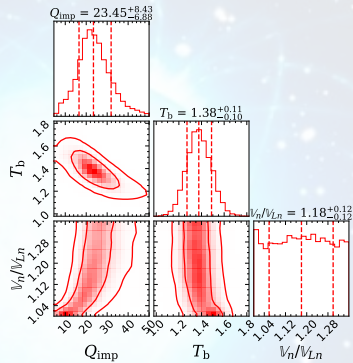
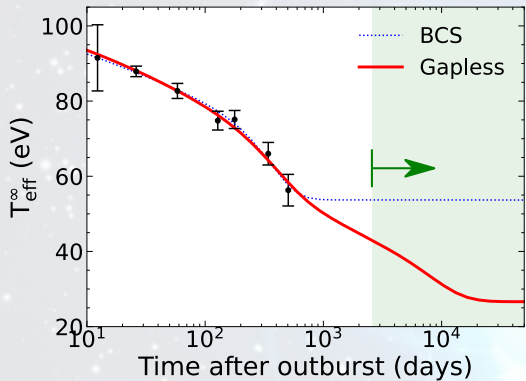
Cooling has been studied with a realistic equation of state of neutron matter based on BSk24 (following Potekhin et al. MNRAS 522:4830–4840 (2023)).



Gapless superfluidity can explain the late-time cooling of MXB 1659–29.

Cooling with thermodynamically consistent EoS

Cooling has been studied with a realistic equation of state of neutron matter based on BSk24 (following Potekhin et al. MNRAS 522:4830–4840 (2023)).



Both BCS and gapless superfluidity provide excellent fit to the cooling data of MXB 1659–29 (outburst II) (but different predictions at late-time).

Conclusions

Microscopic inputs

- Self-Consistent calculations of Δ_q and $\rho_{qq'}$ (entrainment) (Allard and Chamel, Phys. Rev. C. 103, 025804 (2021)).
- Universal relations and approximate expressions (Allard and Chamel, Universe 2021, 7(12), 470).

Conclusions

Microscopic inputs

- Self-Consistent calculations of Δ_q and $\rho_{qq'}$ (entrainment) (Allard and Chamel, Phys. Rev. C 103, 025804 (2021); Chamel and Allard, Phys. Rev. C 100, 06580 (2019)).
- Universal relations and approximate expressions (Allard and Chamel, Universe 2021, 7(12), 470).

Critical quantities for disappearance of superfluidity

- Critical quantities generalized for superfluid mixtures.
- Order parameter ($\propto \Delta_q$) \neq Quasiparticle energy gap \implies Impact on the specific heat (Allard and Chamel, Phys. Rev. C 108, 015801 (2023)) and appearance of a normal fluid (at $T = 0$) (Allard and Chamel, Phys. Rev. C 108, 045801 (2023)).

Conclusions

Neutron star cooling

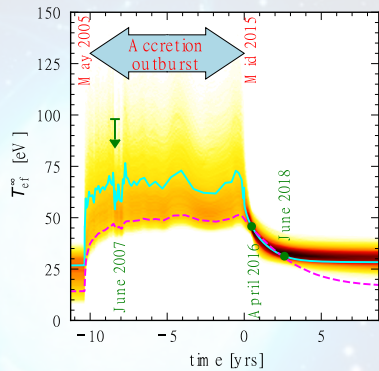
- Gapless superfluidity is compatible with neutron diffusion and with the late-time cooling of KS 1731–260 and MXB 1659–29 (Allard and Chamel, Phys. Rev. Lett. *in press* (2024)).
- Study of KS 1731–260 and MXB 1659–29 with neutron diffusion and gapless superfluidity, for different M_{NS} and R_{NS} pairs and different envelope models (Allard and Chamel, EPJA (2024), *accepted for publication*).

Prospects

Another system exhibits peculiar features

HETE J 1900.1–2455

- Accreted millisecond pulsar:
 $\nu_s = 377.296171971(5)$ Hz.
- **High specific heat required:** "[...] *a significant fraction of the dense core is not superfluid/superconductor.*"
(Degenaar et al., MNRAS 508 (2021))
- But **only 2 observations...**



To clarify

Further observations are expected!

Prospects

Density dependency of V_n and Q_{imp}

Cooling studies were performed assuming a uniform V_n/V_{Ln} and Q_{imp} throughout the crust. More refined studies with different density profiles of V_n (and Q_{imp}) are desirable.

Influence of gapless superfluidity on neutrino emissivities

Influence of gapless superfluidity on neutrino emissivities. Are neutrino cooling channels involving superfluid neutrons still suppressed ?

Prospects

Neutron vortices

Astrophysical manifestations of gapless superfluidity call for further studies of vortex dynamics in neutron star crusts and cores.

Inclusion of rotation: 1D equations \Rightarrow 2D equations

- Beznogov et al., *Astrophys. J.*, 942:72 (2023): NSCool updated to solve fully general relativistic 2D axisymmetric cooling equations (Complex time-dependent evolution of the temperature).
- Ascenzi et al., arXiv:2401.15711 (2024): 3D code designed to study the magneto-thermal evolution of isolated neutron stars.

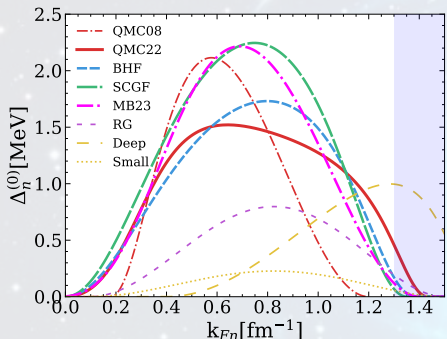
These works are focused on isolated neutron stars: a self-consistent treatment of neutron star cooling and rotation in the context of accreting systems remains to be performed.

Thank you !

Backup slides

1S_0 neutron pairing

Neutron pairing gap computed using various N-body methods:



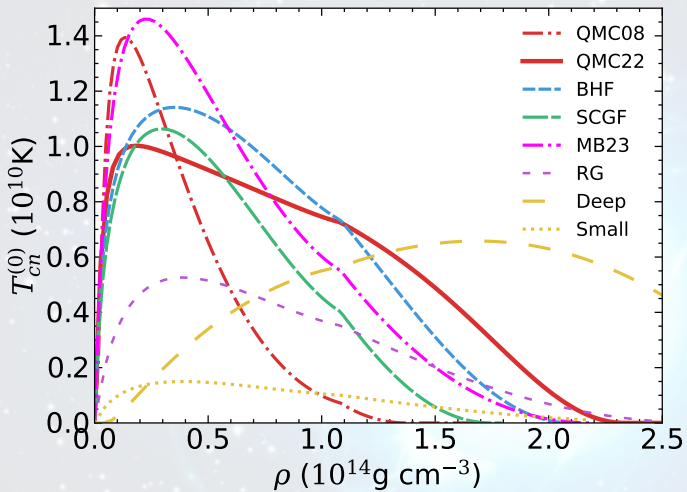
(Dashed box = Fermi wavevectors prevailing in neutron star core)

- **QMC08:** S. Gandolfi et al, Phys. Rev. Lett. **101** (2008).
- **QMC22:** S. Gandolfi et al, Condens. Matter, **7(1)** (2022).
- **BHF:** L. G. Cao et al, Phys. Rev. C **74** (2006).
- **SCGF:** M. Drissi and A. Rios, Eur. Phys. J. A **58** (2022).
- **MB23:** E. Krotscheck et al, arXiv.2305.07096 (2023)
- **Deep and Small:** A. Turlione et al, A&A **577** (2015).

1S_0 neutron pairing

- **RG (Schwenk, Brown et al. 2003):** (One-loop) Renormalization Group equations for PNM. Medium polarization taken into account and self-energy contributions included (in a simple approximation).
- **QMC08 (Gandolfi et al. 2008):** Monte-Carlo computation by solving the many-body problem with a realistic interaction (containing Argonne v_8' (AV8') the two-nucleon interaction and the Urbana IX (UIX) three-nucleon interaction). Medium polarization effects included.
- **QMC22 (Gandolfi et al. 2022):** Most recent Monte-Carlo computation by solving the many-body problem using AV8'+UIX interaction BUT using a better starting trial wavefunction (taking more essential superfluid ground-state correlations into account than it does for QMC08).
- **BHF (Cao et al. 2006):** Brueckner Hartree-Fock computation, considering medium polarization and self-energy effects.
- **SCGF (Drissi et al. 2022):** Pairing gap computed beyond BCS+HF approximation + Three body-forces and medium effects (such as screening terms) and short-range correlations.
- **MB23 (Krotscheck et al.):** Inclusion of many-body effects through diagrammatic methods.

Critical temperatures



Cooling curve

1-to-1 mapping between the cooling curve $T_{\text{eff}}^{\infty}(t)$ and the NS interior.

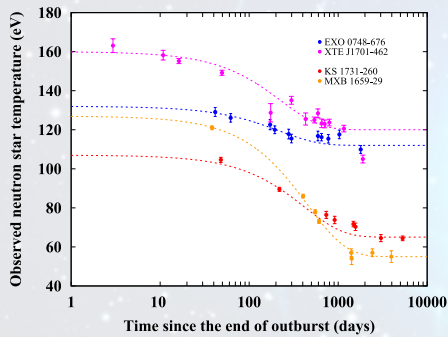
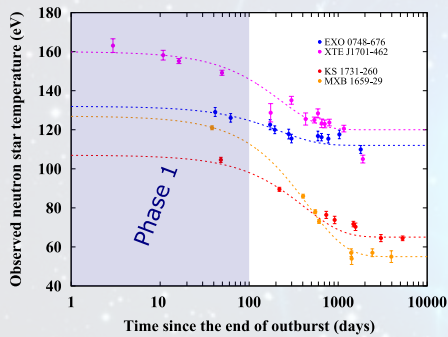


(Figure from R. Wijnands et al, J. Astrophys.
Astr. 38 (2017))

Cooling curve

1-to-1 mapping between the cooling curve $T_{\text{eff}}^{\infty}(t)$ and the NS interior.

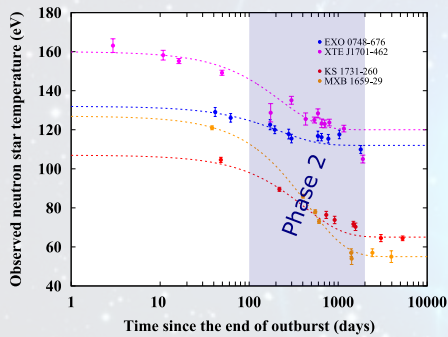


- **Phase 1:** T_{eff}^{∞} sensitive to the outer crust.

(Figure from R. Wijnands et al, J. Astrophys. Astr. 38 (2017))

Cooling curve

1-to-1 mapping between the cooling curve $T_{\text{eff}}^{\infty}(t)$ and the NS interior.



- **Phase 1:** T_{eff}^{∞} sensitive to the outer crust.
- **Phase 2:** T_{eff}^{∞} sensitive to the inner crust.

(Figure from R. Wijnands et al, J. Astrophys. Astr. 38 (2017))

Cooling curve

1-to-1 mapping between the cooling curve $T_{\text{eff}}^{\infty}(t)$ and the NS interior.

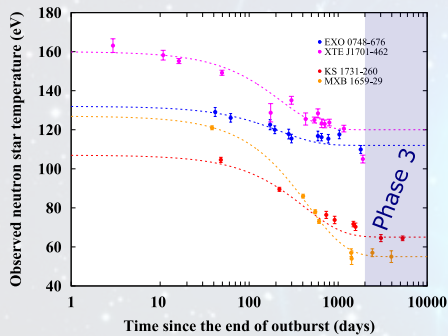


(Figure from R. Wijnands et al, J. Astrophys. Astr. 38 (2017))

- **Phase 1:** T_{eff}^{∞} sensitive to the outer crust.
- **Phase 2:** T_{eff}^{∞} sensitive to the inner crust.
- **Phase 3:** T_{eff}^{∞} sensitive to the outer core \Rightarrow Thermal equilibrium.

The cooling curve allows to probe the NS interiors.

Pinning forces

Pinning forces

Finite V_n can be sustained by the pinning of quantized vortices BUT pinning forces f_{pin} compete against Magnus forces $f_{\text{Magnus}} \implies$ Existence of V_{cr} .

- f_{pin} differs by orders of magnitude.
- Averaging procedure over many vortices and pinning sites (model dependent).
- Vortices can pin to proton fluxons in the core (additional pinning sites: $f_{\text{pin}} \nearrow$).
- Landau's velocity can be suppressed significantly by the presence of clusters (Miller et al., Phys. Rev. Lett. 99, 070402 (2007)).

Astrophysical manifestations of gapless superfluidity call for further studies of vortex dynamics in neutron star crusts and cores.

Estimates of V_{cr}

The lag $\mathbb{V}_n \simeq V_n$ is limited by the critical lag V_{cr} beyond which vortices are unpinned.

- Melatos & Millhouse, ApJ, 948(2), 106 (2023) (Statistical analysis of 541 glitches and 177 pulsars): $V_{\text{cr}} \sim 10^5 \text{ cm s}^{-1}$ BUT no pinning in the core.
- Pizzochero, ApJL 743(1), 20 (2011) (straight parallel vortices pinned to the crust):

$$V_{\text{cr}} \approx 10^7 (f_p / 10^{18} \text{ dyn cm}^{-1}) \text{ cm s}^{-1},$$

where f_p is the maximum mesoscopically averaged pinning force per unit length.

The theoretical challenges to estimate this force are numerous (see, e.g., Antonopoulou et al., Rep. Prog. Phys. 85(12), 126901 (2022), for a recent review).

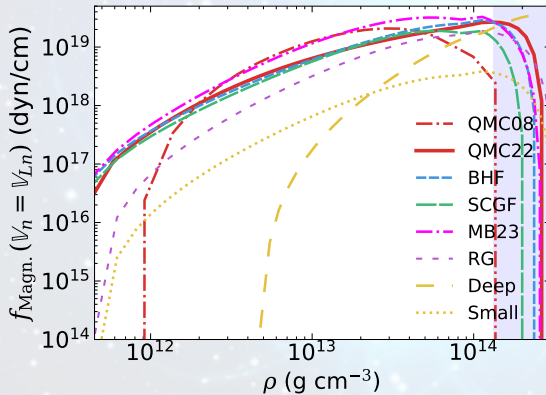
Computing f_p

- Pecak et al., Phys. Rev. C 104, 055801 (2021): internal quantum structure of a vortex locally modified in presence of nuclear clusters \Rightarrow a vortex should be described within a fully self-consistent quantum mechanical approach.
- Klausner et al., Phys. Rev. C 108, 035808 (2023): pinning force (for one single cluster) traditionally determined from static calculations of energy differences.
- Wlazlowski et al., Phys. Rev. Lett. 117(23), 232701 (2016): A more reliable approach consists in calculating the force dynamically BUT no such calculations have been systematically carried out so far !
- Calculations on a mesoscopic scale are more uncertain: results depend on the vortex tension and crustal structure (see, Seveso et al., MNRAS 455(4), 3952–3967 (2016) and Link and Levin, Astrophys. J. 941(2), 148 (2022)). **Estimates of f_p differ by orders of magnitude.**
- Vortices are also expected to pin to proton fluxoids in the deepest layers of the crust or, even, in the core ! (pinning to fluxoids is supported by observations of Crab and Vela pulsar glitches, Sourie and Chamel, MNRAS 493(1), 98–102 (2020)).

Pinning force estimation

The pinning force can be roughly estimated from the Magnus force.

$$f_p(\rho) \approx 2.5 \times 10^{19} \text{ dyn cm}^{-1} \left(\frac{\Delta_n^{(0)}}{1 \text{ MeV}} \right) \left(\frac{\rho Y_{\text{nf}}}{10^{14} \text{ g cm}^{-3}} \right)^{2/3}. \quad (1)$$



Inhomogeneities in the crust and V_{cr}

We can adopt the estimate $f_p \simeq 10^{18} \text{ dyn cm}^{-1}$ (also given in Antonopoulou et al., Rep. Prog. Phys. 85(12), 126901 (2022)) which yields (using the *snowplow model*) $V_{\text{cr}} \sim 10^7 \text{ cm s}^{-1}$.

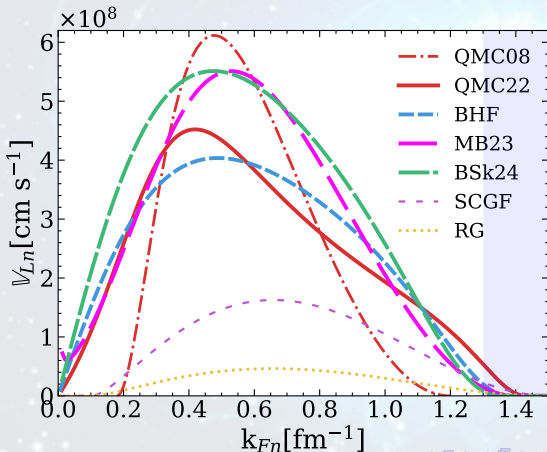
- Landau's velocity $\mathbb{V}_{Ln} \sim 10^8 \text{ cm s}^{-1}$ is one order of magnitude higher than V_{cr} .
- However, the estimates of V_{cr} , \mathbb{V}_{Ln} , and f_p were obtained ignoring the inhomogeneities in the crust.
- Antonelli et al., MNRAS 464(1), 721–733 (2017): crust inhomogeneities increase V_{cr} by a factor $(1 - \varepsilon_n) = m_n^*/m_n$ (with being ε_n = entrainment parameter and m_n^*/m_n = dynamical effective mass).
- Chamel, Phys. Rev. C 85(3), 035801 (2012): $m_n^*/m_n \approx 1 - 14$ (depending on the crustal layer) \implies the maximum V_{cr} could be increased by an order of magnitude !

Having $\mathbb{V}_{Ln} \lesssim V_{\text{cr}}$ is not implausible !

Landau's velocity in neutron matter

Landau's velocity is approximately given by

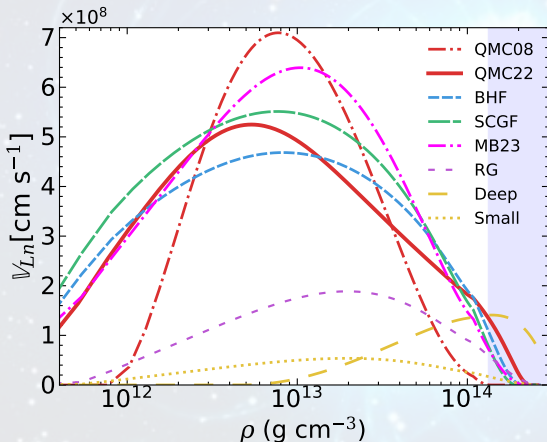
$$\mathbb{V}_{Ln} \approx 1.2 \times 10^8 \text{ cm s}^{-1} \left(\frac{\Delta_n^{(0)}}{1 \text{ MeV}} \right) \left(\frac{10^{14} \text{ g cm}^{-3}}{\rho Y_{\text{nf}}} \right)^{1/3}. \quad (2)$$



Landau's velocity in neutron matter

Landau's velocity is approximately given by

$$V_{Ln} \approx 1.2 \times 10^8 \text{ cm s}^{-1} \left(\frac{\Delta_n^{(0)}}{1 \text{ MeV}} \right) \left(\frac{10^{14} \text{ g cm}^{-3}}{\rho Y_{\text{nf}}} \right)^{1/3}. \quad (2)$$

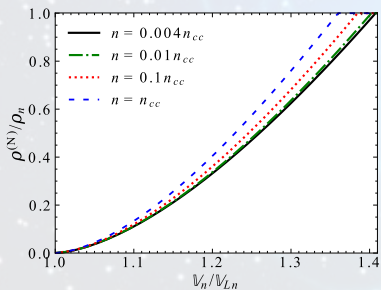


Magnus force in gapless superfluidity

The Magnus force depends on the superfluid density (see, for e.g.; Antonelli et al., In Astrophysics in the XXI Century with Compact Stars, Chap. 7, p219-281 (2022))

$$f_{\text{pin}} \simeq \kappa_n (\rho_n - \rho_n^{(N)}) \mathbb{V}_n .$$

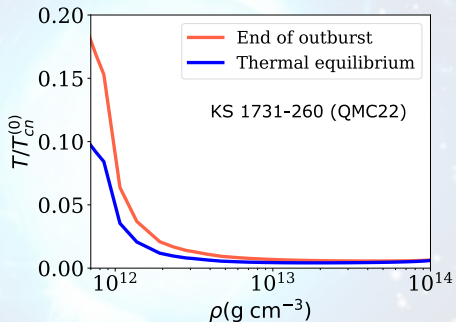
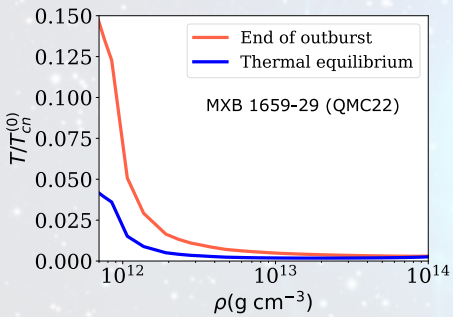
The normal neutron density $\rho_n^{(N)}$ is defined in terms of the entrainment matrix (Allard and Chamel, Phys. Rev. C. 108, 045801 (2023)).



- $\rho_n^{(N)} \rightarrow \rho_n$ with increasing \mathbb{V}_n .
- **Reduction of the pinning force** for increasing \mathbb{V}_n in gapless superfluidity.

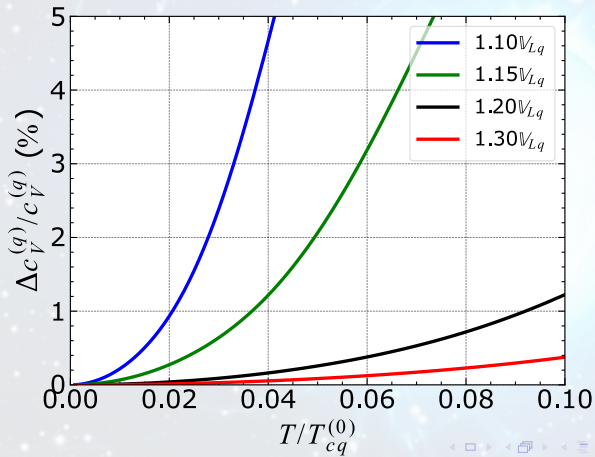
Low-temperature approximation ?

Highest temperatures reached at $\sim 0.15 - 0.20 T_{cn}^{(0)}$, at the end of outburst in the shallowest regions of the crust.



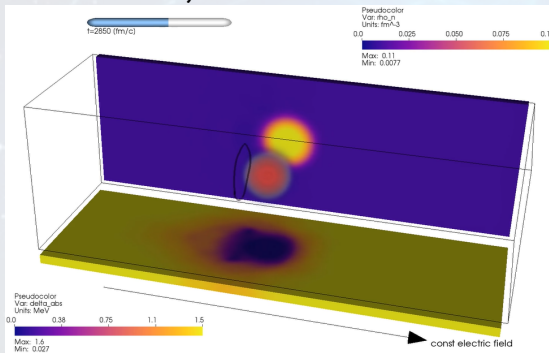
Low-temperature approximation ?

(Relative) errors not exceeding 2.9% (for MXB) and 0.028% (for KS) in shallowest regions. For the deeper layers, errors do not exceed 0.01% !



Stability of gapless superfluidity

Warsaw' simulations highlight the appearance of a vortex ring past a (normal) nucleus for velocities beyond $V_{\text{ring}} \sim V_{L_n}$ and $\xi_n \ll L = \text{Nucleus size} \implies$
Instability ?



Similar criteria have also been found in the context of (terrestrial) superconductors ! A. Schmid, J. Low. Temp. Phys., 1 (1969)

Stability of gapless superfluidity

Stable or not stable ?

- Autti et al., Phys. Rev. Research 2, 033013 (2020): Gapless regime also studied in condensed matter and it was found to be stable !
- Biswanath et al., Phys. Rev. D 107, 023004 (2023): Normal neutrons produced by Cooper pair breaking (in gapless regime) are expected to be scattered with the vortex core normal neutrons \Rightarrow Unpinning of a large number of vortices, resulting to a pulsar glitch !

Energy-density functional theory with currents

The dynamic of neutron-proton mixtures is governed by the **time-dependent Hartree-Fock Bogoliubov (TDHFB) equations**

$$i\hbar\partial_t n_q(\mathbf{r}\sigma, \mathbf{r}'\sigma', t) = h_q(\mathbf{r}, t)n_q(\mathbf{r}\sigma, \mathbf{r}'\sigma', t) - h_q^*(\mathbf{r}', t)\tilde{n}_q(\mathbf{r}\sigma, \mathbf{r}'\sigma', t) \\ + \sigma\sigma'\tilde{\Delta}_q(\mathbf{r}, t)\tilde{n}_q(\mathbf{r} - \sigma, \mathbf{r}' - \sigma', t) - \tilde{n}_q(\mathbf{r}\sigma, \mathbf{r}'\sigma', t)\tilde{\Delta}_q^*(\mathbf{r}', t)$$

with single-particle hamiltonian (depending on densities, **effective mass** and **currents**)

$$h_q(\mathbf{r}, t) = -\nabla \cdot \frac{\hbar^2}{2m_q^\oplus(\mathbf{r}, t)}\nabla + U_q(\mathbf{r}, t) + \frac{1}{2i} [\mathbf{I}_q(\mathbf{r}, t) \cdot \nabla + \nabla \cdot \mathbf{I}_q(\mathbf{r}, t)]$$

with potentials defined through particle density $n_q(\mathbf{r}\sigma, \mathbf{r}'\sigma', t)$ and pair density matrices $\tilde{n}_q(\mathbf{r}\sigma, \mathbf{r}'\sigma', t)$,

$$\frac{\hbar^2}{2m_q^\oplus(\mathbf{r}, t)} = \frac{\delta E}{\delta \tau_q(\mathbf{r}, t)}, \quad U_q(\mathbf{r}, t) = \frac{\delta E}{\delta n_q(\mathbf{r}, t)}, \quad \mathbf{I}_q(\mathbf{r}, t) = \frac{\delta E}{\delta \mathbf{j}_q(\mathbf{r}, t)},$$

$$\tilde{\Delta}_q(\mathbf{r}, t) = \Delta_q(\mathbf{r}, t)e^{i\phi_q(\mathbf{r}, t)} = 2\frac{\delta E}{\delta \tilde{n}_q^\star(\mathbf{r}, t)}.$$

Mass currents

A **continuity equation** can be derived from the TDHFB equations (Allard and Chamel in Phys. Rev. C. 100, 065801 (2019) and Phys. Rev. C. 103, 025804 (2021))

$$\partial_t (m_q n_q(\mathbf{r}, t)) + \nabla \cdot \boldsymbol{\rho}_q(\mathbf{r}, t) = 0$$

Mass current $\boldsymbol{\rho}_q$

$$\boldsymbol{\rho}_q(\mathbf{r}, t) = m_q n_q(\mathbf{r}, t) \left(\frac{\hbar \mathbf{j}_q(\mathbf{r}, t)}{m_q^\oplus(\mathbf{r}, t) n_q(\mathbf{r}, t)} + \frac{\mathbf{I}_q(\mathbf{r}, t)}{\hbar} \right) = m_q n_q(\mathbf{r}, t) \mathbf{v}_q(\mathbf{r}, t)$$

Which allows to define the **true velocity** as $\mathbf{v}_q(\mathbf{r}, t) = \boldsymbol{\rho}_q(\mathbf{r}, t) / (m_q n_q(\mathbf{r}, t))$

- Does not explicitly depend on the pairing gap $\widetilde{\Delta}_q$.
- **General** case: valid for both uniform and non-uniform systems.

Homogeneous solutions: finite T and finite currents

Focusing on hot **homogeneous neutron-proton superfluid mixture** with stationary flows in normal fluid rest frame ($\mathbf{v}_N = \mathbf{0}$), **TDHFB can be solved exactly** (Allard and Chamel, Phys. Rev. C. 103, 025804 (2021)) !

$$\mathcal{E}_{\mathbf{k}}^{(q)} = \hbar \mathbf{k} \cdot \mathbb{V}_{\mathbf{q}} + \sqrt{\varepsilon_{\mathbf{k}}^{(q)2} + \Delta_q^2}, \quad \varepsilon_{\mathbf{k}}^{(q)} = \frac{\hbar^2 \mathbf{k}^2}{2m_q^{\oplus}} - \mu_q,$$

Effective superfluid velocity

$$\mathbb{V}_{\mathbf{q}} = \frac{m}{m_q^{\oplus}} \mathbf{V}_{\mathbf{q}} + \frac{\mathbf{I}_{\mathbf{q}}}{\hbar} \neq \mathbf{v}_{\mathbf{q}}$$

- $\mathbb{V}_{\mathbf{q}}$ contains the mutual contributions of \mathbf{V}_n and \mathbf{V}_p .
- **Dynamical decoupling** between quantities associated with protons or neutrons.

Homogeneous solutions: $T = 0$ K and small currents

For homogeneous neutron-proton superfluid mixture, **at low temperatures and small currents**, the normal component disappears ($\mathbf{v}_N = 0$)

$$\rho_n = \rho_{nn}^{(\text{TDHF})} \mathbf{V}_n + \rho_{np}^{(\text{TDHF})} \mathbf{V}_p, \quad \rho_p = \rho_{pp}^{(\text{TDHF})} \mathbf{V}_p + \rho_{pn}^{(\text{TDHF})} \mathbf{V}_n$$

The entrainment matrix becomes **independent of pairing** \Rightarrow TDHF !

(Chamel and Allard, Phys. Rev. C 100, 065801 (2019))

$$\rho_{np}^{(\text{TDHF})} = \rho_{pn}^{(\text{TDHF})} = \frac{1}{4} mn(1 - \eta^2) \left(1 - \frac{\mathbf{m}}{\mathbf{m}_V^\oplus} \right)$$

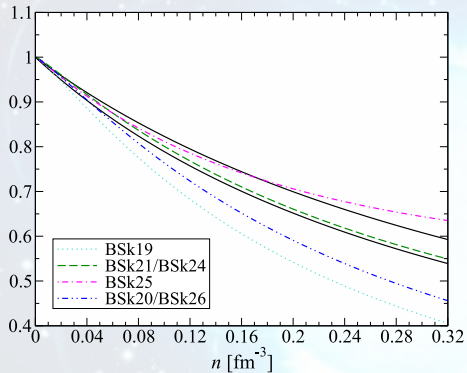
$$\rho_{nn}^{(\text{TDHF})} = \frac{1}{2} mn(1 + \eta) - \rho_{np}^{(\text{TDHF})}, \quad \rho_{pp}^{(\text{TDHF})} = \frac{1}{2} mn(1 - \eta) - \rho_{np}^{(\text{TDHF})}.$$

with $n = (n_n + n_p)$ the total density and $\eta = (n_n - n_p)/n$ the isospin asymmetry.

The entrainment matrix is parametrized by the **isovector effective mass**!

Homogeneous solutions: $T = 0$ K and small currents

Isovector effective mass is also related to **giant resonances in atomic nuclei !**



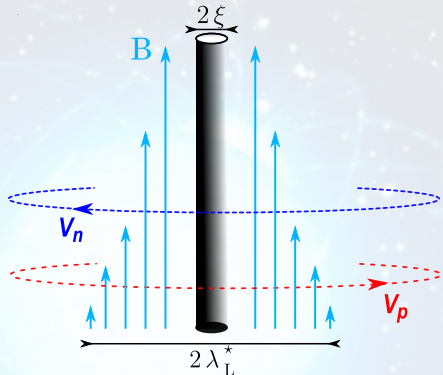
Its density dependence is still uncertain !

Influence of entrainment effects in pulsars

- Induced circulation of protons around neutron vortices.
- Neutron vortices carry a magnetic flux Φ^* ($T = 0$ and $\nabla_q \leq \nabla_{Lq}$):

$$\Phi^* = \frac{hc}{2|e|} \frac{\rho_{np}}{\rho_{pp}} .$$

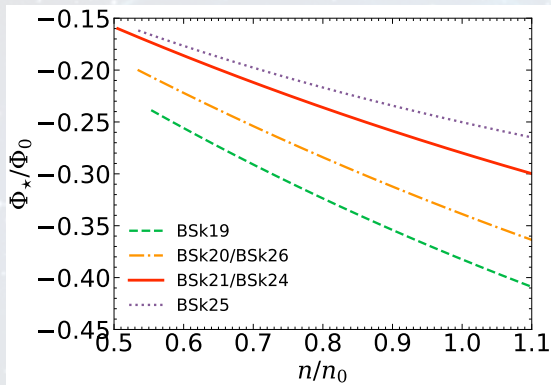
(Sedrakyan and Shakhabasyan,
Astrofizika 8, 557 (1972); ibid. 16, 727
(1980))



Electrons scattering off the induced magnetic flux, strong coupling between the core superfluid and the crust (Alpar, Langer, Sauls, ApJ 282, 533 (1984)).

Neutron vortex magnetization

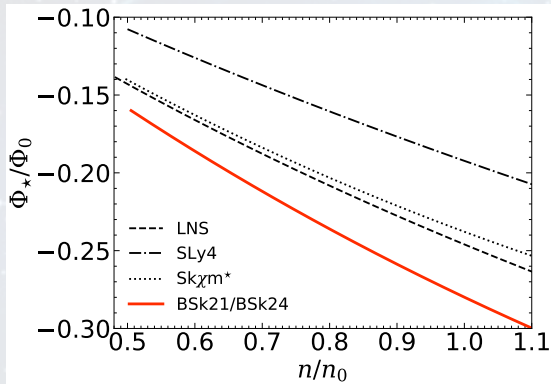
Exact solution for zero temperature and small currents ($\mathbb{V}_q \leq \mathbb{V}_{Lq}$).



For $T \neq 0$ or higher velocities (i.e. $\mathbb{V}_q > \mathbb{V}_{Lq}$), computing the vortex magnetic flux Φ^* involves additional contributions coming from the normal fluid.

Neutron vortex magnetization

Exact solution for zero temperature and small currents ($\mathbb{V}_q \leq \mathbb{V}_{Lq}$).



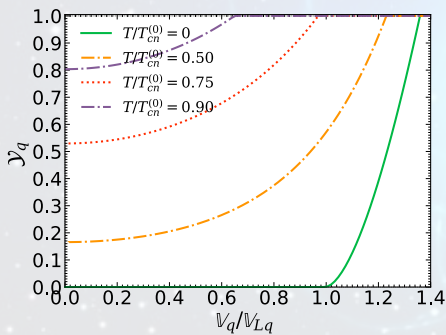
For $T \neq 0$ or higher velocities (i.e. $\mathbb{V}_q > \mathbb{V}_{Lq}$), computing the vortex magnetic flux Φ^* involves additional contributions coming from the normal fluid.

Mass current and generalized Yosida functions

The true velocity (and mass current) takes a simple form

$$\mathbf{v}_q = \left(1 - \mathcal{Y}_q(T, \mathbb{V}_q)\right) \mathbb{V}_q$$

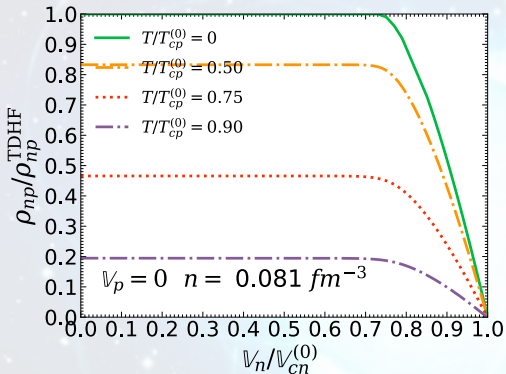
With \mathcal{Y}_q , the **generalized Yosida functions** (universal after using \mathbb{V}_q and rescaling)



Interpolating functions available
(Allard and Chamel, Universe 7(12) (2021)) !

Entrainment matrix: finite T and finite currents

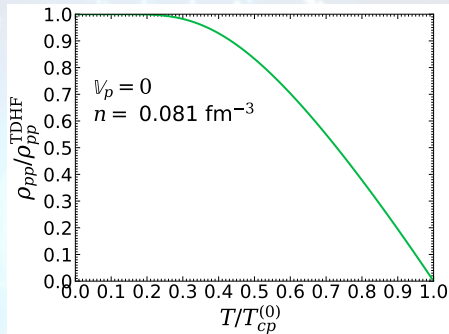
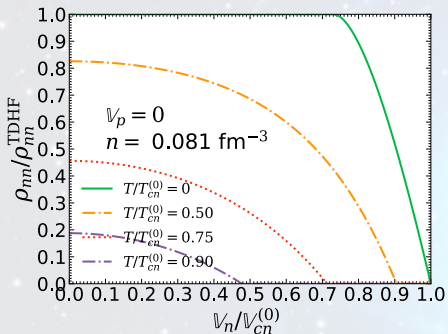
Entrainment matrix numerically computed in Allard and Chamel, Universe 7(12) (2021) (Protons coupled with the rest of the star: $v_p = \nabla_p = 0$).



Generalization of the **superfluid mass densities** for mixtures !

Entrainment matrix: finite T and finite currents

Entrainment matrix numerically computed in Allard and Chamel, Universe 7(12) (2021) (Protons coupled with the rest of the star: $\nu_p = \mathbb{V}_p = 0$).

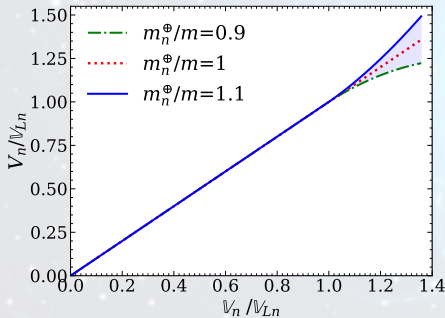


Generalization of the **superfluid mass densities** for mixtures !

Velocities

Three kind of velocities

- Superfluid velocity V_q : Rescaled **momentum**.
- Effective superfluid velocity \mathbb{V}_q : **Dynamical decoupling** between neutrons and protons.
- True velocity v_q : Velocity of **mass-transport** of nucleons.

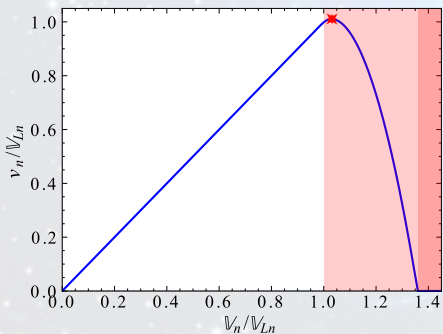


Example: Results obtained from neutron matter ($n_p = 0$) \Rightarrow
Non-linear universal relations
(beyond Landau's velocity)!

Velocities

Three kind of velocities

- Superfluid velocity V_q : Rescaled **momentum**.
- Effective superfluid velocity \mathbb{V}_q : **Dynamical decoupling** between neutrons and protons.
- True velocity v_q : Velocity of **mass-transport** of nucleons.



Example: neutron matter

Non-linear universal relations
(beyond Landau's velocity)!

crustcool code

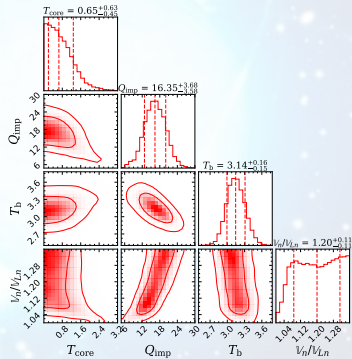
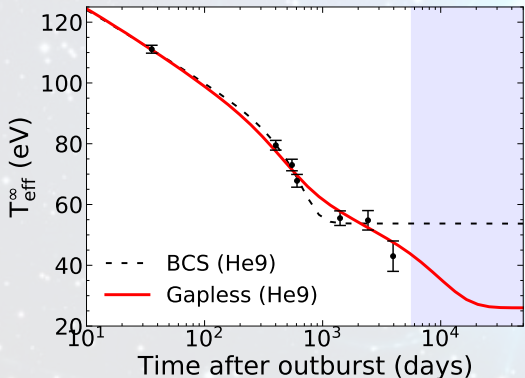
- **Composition:** Haensel & Zdunik, A&A 229 (1990).
- **Thermal conductivity:** Fortran subroutine `condegin` (Potekhin, <http://www.ioffe.ru/astro/conduct/condin.html>).
- **Pressure :** Degenerate et relativistic electrons (Paczynski ApJ 267 (1983)) + Non-relativistic degenerate neutrons (Mackie & Baym, Nucl. Phys. A 285 (1977)) + Ionic and radiative pressures neglected.
- **Specific heat:** Electrons in normal phase + Gapless neutrons (Fermi energy from Mackie & Baym, Nucl. Phys. A 285 (1977)) + Ionic contribution (solid ions, G. Chabrier, ApJ 414 (1993)).

Last observation point of MXB 1659–29 (outburst I)

Results obtained for Haensel & Zdunik (1990) with neutron diffusion.

Cooling of MXB 1659–29 (outburst I)

Four possible values for the last data point: $k_B T_{\text{eff}}^{\infty} = 43 \pm 5$ eV.

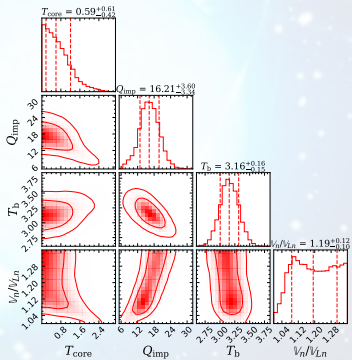
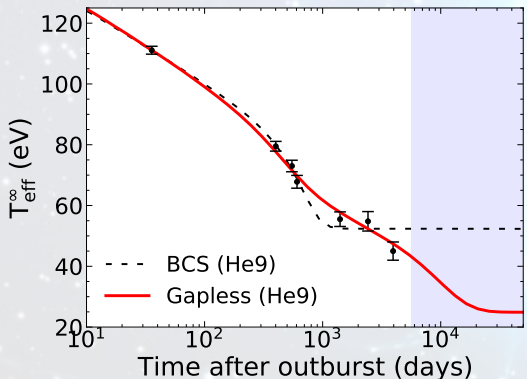


Last observation point of MXB 1659–29 (outburst I)

Results obtained for Haensel & Zdunik (1990) with neutron diffusion.

Cooling of MXB 1659–29 (outburst I)

Four possible values for the last data point: $k_B T_{\text{eff}}^{\infty} = 45 \pm 3$ eV.

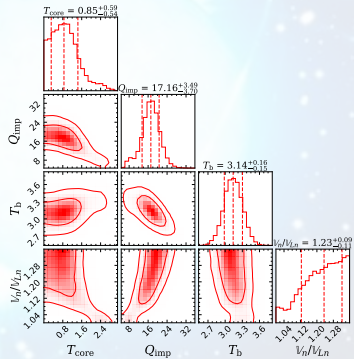
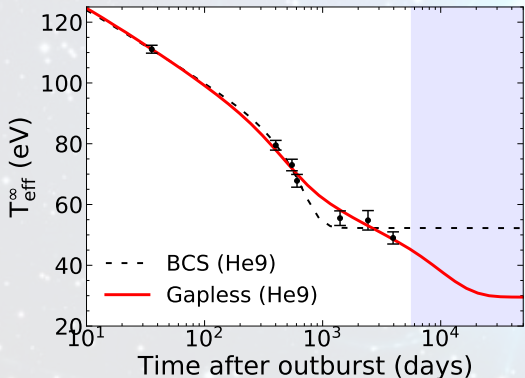


Last observation point of MXB 1659–29 (outburst I)

Results obtained for Haensel & Zdunik (1990) with neutron diffusion.

Cooling of MXB 1659–29 (outburst I)

Four possible values for the last data point: $k_B T_{\text{eff}}^{\infty} = 49 \pm 2$ eV.

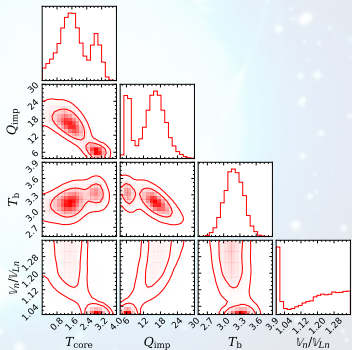
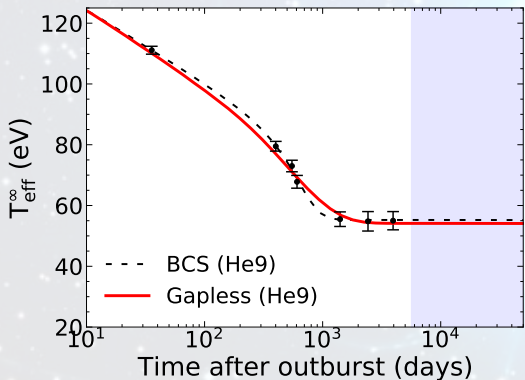


Last observation point of MXB 1659–29 (outburst I)

Results obtained for Haensel & Zdunik (1990) with neutron diffusion.

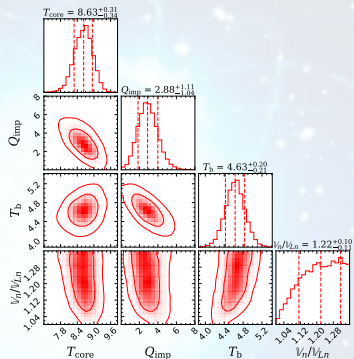
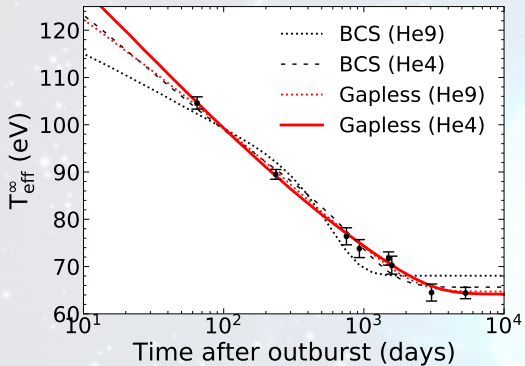
Cooling of MXB 1659–29 (outburst I)

Four possible values for the last data point: $k_B T_{\text{eff}}^{\infty} = 55 \pm 3$ eV.



Cooling with accreted-crust EoS BSk21 (no nHD)

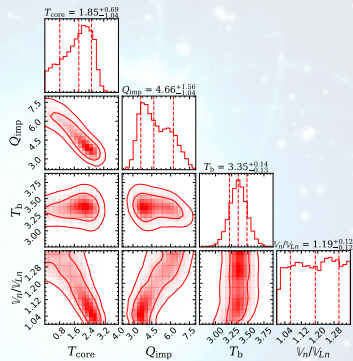
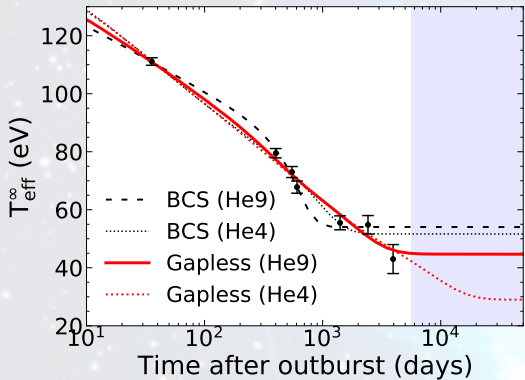
Cooling has been studied with the accreted-crust EoS from Fantina et al. A&A 620, A105 (2018) based on (BSk21).



Gapless superfluidity gives an excellent fit to the cooling data.

Cooling with accreted-crust EoS BSk21 (no nHD)

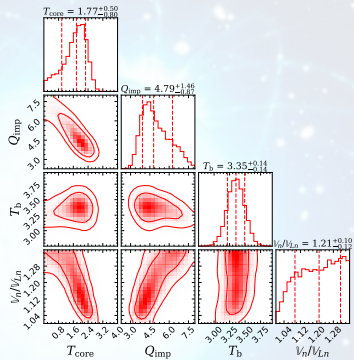
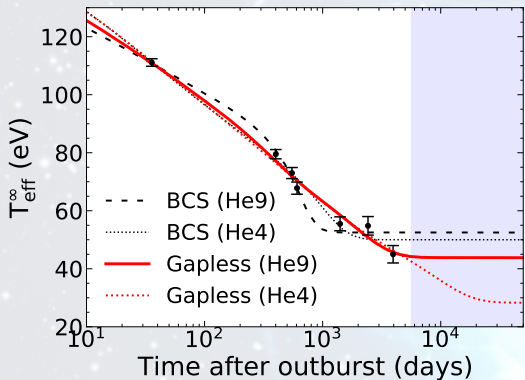
Cooling has been studied with the accreted-crust EoS from Fantina et al. A&A 620, A105 (2018) based on (BSk21).



Gapless superfluidity gives a good fit to the cooling data, for the last point at 43 ± 5 eV.

Cooling with accreted-crust EoS BSk21 (no nHD)

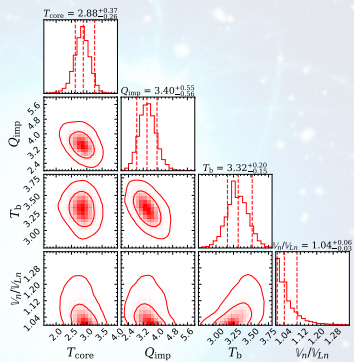
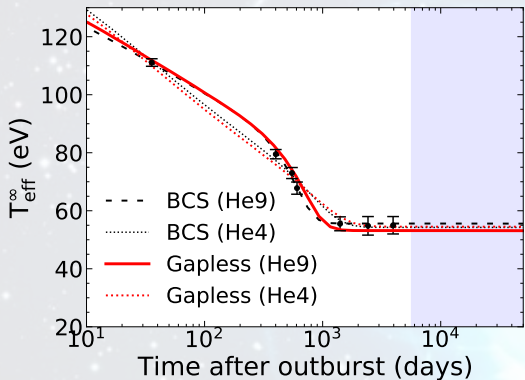
Cooling has been studied with the accreted-crust EoS from Fantina et al. A&A 620, A105 (2018) based on (BSk21).



Gapless superfluidity gives a good fit to the cooling data, for the last point at 45 ± 3 eV.

Cooling with accreted-crust EoS BSk21 (no nHD)

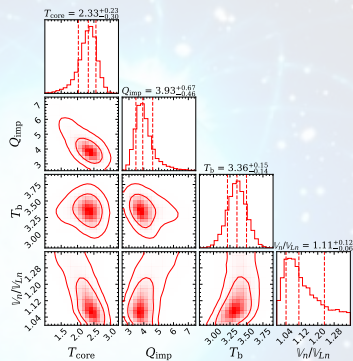
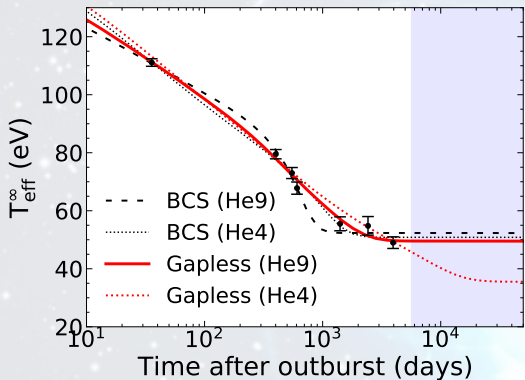
Cooling has been studied with the accreted-crust EoS from Fantina et al. A&A 620, A105 (2018) based on (BSk21).



Gapless superfluidity gives a good fit to the cooling data, for the last point at 55 ± 3 eV.

Cooling with accreted-crust EoS BSk21 (no nHD)

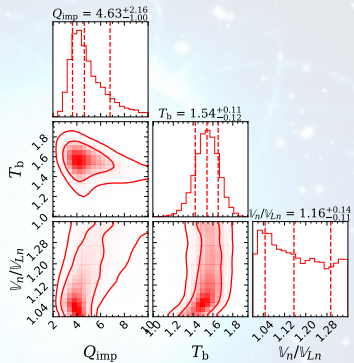
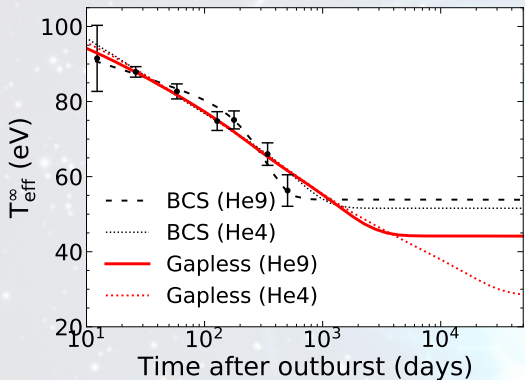
Cooling has been studied with the accreted-crust EoS from Fantina et al. A&A 620, A105 (2018) based on (BSk21).



Gapless superfluidity gives a good fit to the cooling data, for the last point at 49 ± 2 eV.

Cooling with accreted-crust EoS BSk21 (no nHD)

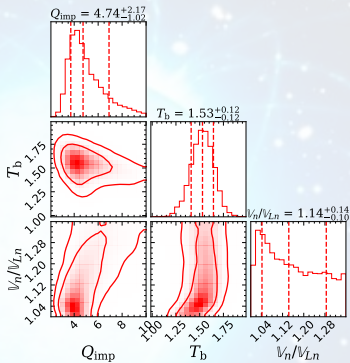
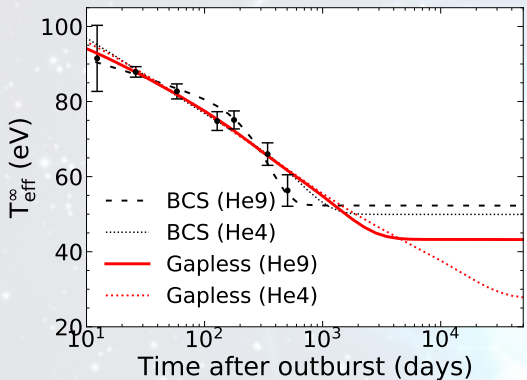
Cooling has been studied with the accreted-crust EoS from Fantina et al. A&A 620, A105 (2018) based on (BSk21).



Gapless superfluidity slightly misses the last data point.

Cooling with accreted-crust EoS BSk21 (no nHD)

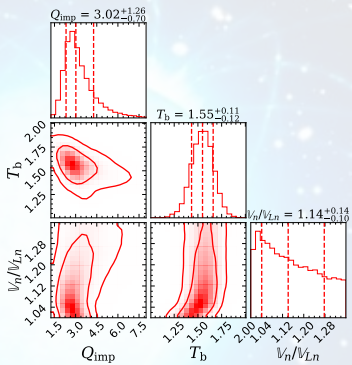
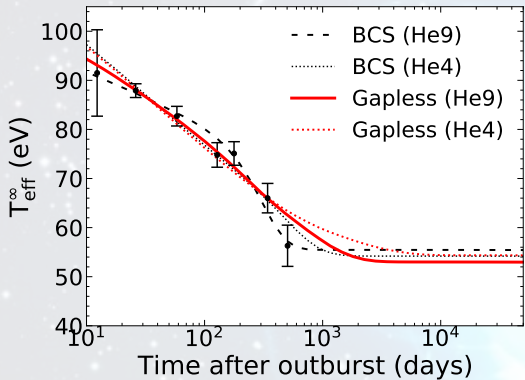
Cooling has been studied with the accreted-crust EoS from Fantina et al. A&A 620, A105 (2018) based on (BSk21).



Gapless superfluidity slightly misses the last data point.

Cooling with accreted-crust EoS BSk21 (no nHD)

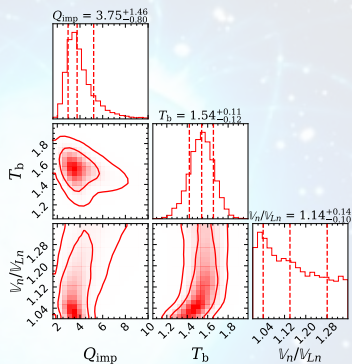
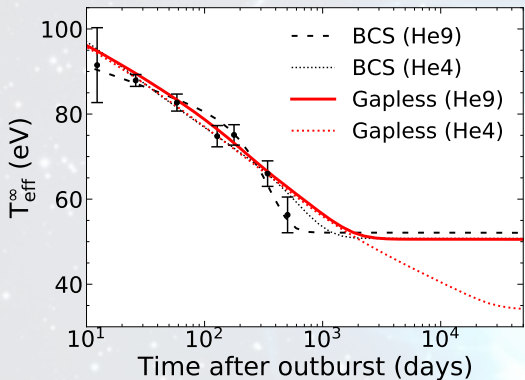
Cooling has been studied with the accreted-crust EoS from Fantina et al. A&A 620, A105 (2018) based on (BSk21).



Gapless superfluidity slightly misses the last data point.

Cooling with accreted-crust EoS BSk21 (no nHD)

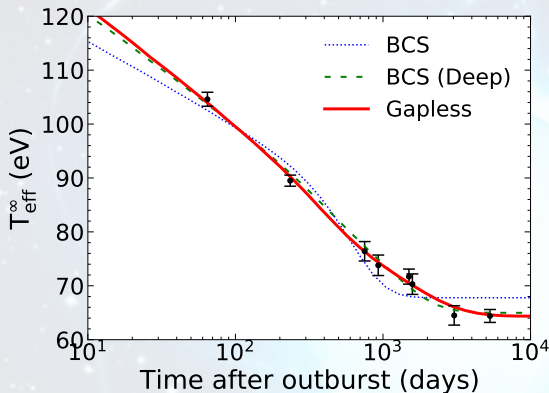
Cooling has been studied with the accreted-crust EoS from Fantina et al. A&A 620, A105 (2018) based on (BSk21).



Gapless superfluidity slightly misses the last data point.

Influence of the Deep gap

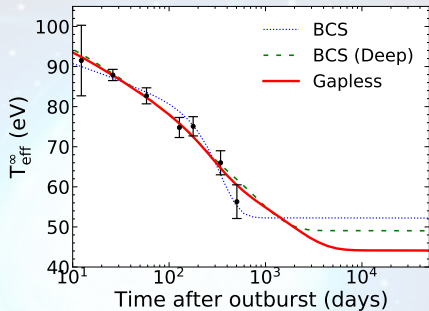
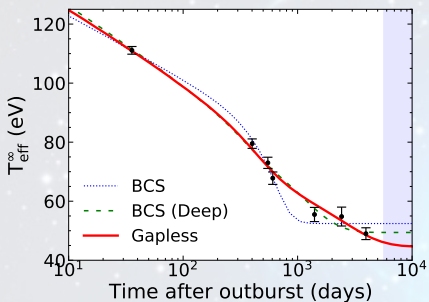
Study of the deep gap (using Haensel & Zdunik (1990), without nHD with He9 envelope model) and $M_{\text{NS}} = 1.62M_{\odot}$ and $R_{\text{NS}} = 11.2 \text{ km}$.



Deep gap (with BCS superfluidity) gives good fit to the cooling data.

Influence of the Deep gap

Study of the deep gap (using Haensel & Zdunik (1990), without nHD with He9 envelope model) and $M_{\text{NS}} = 1.62M_{\odot}$ and $R_{\text{NS}} = 11.2 \text{ km}$.



Deep gap (with BCS superfluidity) gives good fit to the cooling data.